Molecular Therapy
Methods & Clinical Development
Original Article

Long-term correction of ornithine transcarbamylase deficiency in Spf-Ash mice with a translationally optimized AAV vector

Giulia De Sabbata,[1] Florence Boisgerault,[2,3] Corrado Guarnaccia,[1] Alessandra Iaconcig,[1] Giulia Bortolussi,[1] Fanny Collaud,[2,3] Giuseppe Ronzitti,[2,3] Marcelo Simon Sola,[2,3] Patrice Vidal,[2,3] Jeremy Rouillon,[2,3] Severine Charles,[2,3] Emanuele Nicastro,[4] Lorenzo D'Antiga,[4] Petr Ilyinskii,[5] Federico Mingozzi,[2,3,6] Takashi Kei Kishimoto,[5] and Andrés F. Muro[1]

[1]International Center for Genetic Engineering and Biotechnology (ICGEB), 34149 Trieste, Italy; [2]Généthon, 91000 Evry, France; [3]Université Paris-Saclay, Université Evry, INSERM, Généthon, Integrare Research Unit UMR_S951, 91000 Evry, France; [4]Ospedale Papa Giovanni XXIII, 24127 Bergamo, BG, Italy; [5]Selecta Biosciences, Watertown, MA 02472, USA; [6]Institut de Myologie, 73013 Paris, France

Ornithine transcarbamylase deficiency (OTCD) is an X-linked liver disorder caused by partial or total loss of OTC enzyme activity. It is characterized by elevated plasma ammonia, leading to neurological impairments, coma, and death in the most severe cases. OTCD is managed by combining dietary restrictions, essential amino acids, and ammonia scavengers. However, to date, liver transplantation provides the best therapeutic outcome. AAV-mediated gene-replacement therapy represents a promising curative strategy. Here, we generated an AAV2/8 vector expressing a codon-optimized human *OTC* cDNA by the α1-AAT liver-specific promoter. Unlike standard codon-optimization approaches, we performed multiple codon-optimization rounds via common algorithms and ortholog sequence analysis that significantly improved mRNA translatability and therapeutic efficacy. AAV8-hOTC-CO (codon optimized) vector injection into adult OTC$^{Spf\text{-}Ash}$ mice (5.0E11 vg/kg) mediated long-term complete correction of the phenotype. Adeno-Associated viral (AAV) vector treatment restored the physiological ammonia detoxification liver function, as indicated by urinary orotic acid normalization and by conferring full protection against an ammonia challenge. Removal of liver-specific transcription factor binding sites from the AAV backbone did not affect gene expression levels, with a potential improvement in safety. These results demonstrate that AAV8-hOTC-CO gene transfer is safe and results in sustained correction of OTCD in mice, supporting the translation of this approach to the clinic.

INTRODUCTION

Inherited metabolic disorders affecting the urea cycle can trigger severe hyperammonemia, with the risk of permanent cognitive impairment, coma, and death.[1] Urea cycle disorders account for about 1 every 8,000 births worldwide.[2,3] Ornithine transcarbamylase deficiency (OTCD) is the most common cause of urea cycle disorders, with a worldwide incidence estimated between 1:17,000 to 1:60,000 live births.[4,5] Mutations in the X-linked *OTC* gene reduce or ablate OTC function, resulting in the impairment of urea production and accumulation of neurotoxic ammonium, glutamine, and other amino acids, and increased excretion of urinary orotic acid. Complete deficiency of OTC results in the most severe form of the disease, which presents in the first days of life and is associated with permanent neurological impairment and high mortality.[6] In milder forms, the symptoms may manifest later in life, with altered neurocognitive status, reduced consciousness, and lethargy. OTCD can be managed with a low-protein diet combined with ammonia scavengers, which activate alternative nitrogen clearance pathways, but does not prevent hyperammonemic crises.[6,7] The only curative treatment for OTCD is liver transplantation, a procedure that may have substantial morbidity and mortality, is limited by the availability of compatible donor organs, and requires life-long immunosuppression to avoid organ rejection.[8–10]

Liver-directed gene therapy mediated by recombinant adeno-associated viral (rAAV) vectors holds great promise in treating adult patients suffering from monogenic diseases of the liver.[11–14] The potential of adeno-associated virus (AAV)-based gene therapy to correct the OTCD phenotype has been demonstrated in the OTC$^{Spf\text{-}Ash}$ mouse model,[15–18] but a clinically approved gene-therapy product to treat OTCD is still lacking. AAV8 was previously demonstrated to be very efficient in liver transduction in rodents and non-human primates, with clinical trials confirming the safety of the vector.[11–14] However, despite the non-integrative nature of AAV, concerns about the potential insertional mutagenesis and tumorigenesis mediated by AAV vectors are a matter of debate.[19–23] For example, it has been recently reported that fragments of AAV wild-type (WT) genomes were found integrated in the proximity of known cancer-related genes and were possibly associated with the development of hepatocellular

Received 9 July 2020; accepted 11 November 2020;
https://doi.org/10.1016/j.omtm.2020.11.005.

Correspondence: Andrés F. Muro, International Center for Genetic Engineering and Biotechnology (ICGEB), 34149 Trieste, TS, Italy.
E-mail: muro@icgeb.org

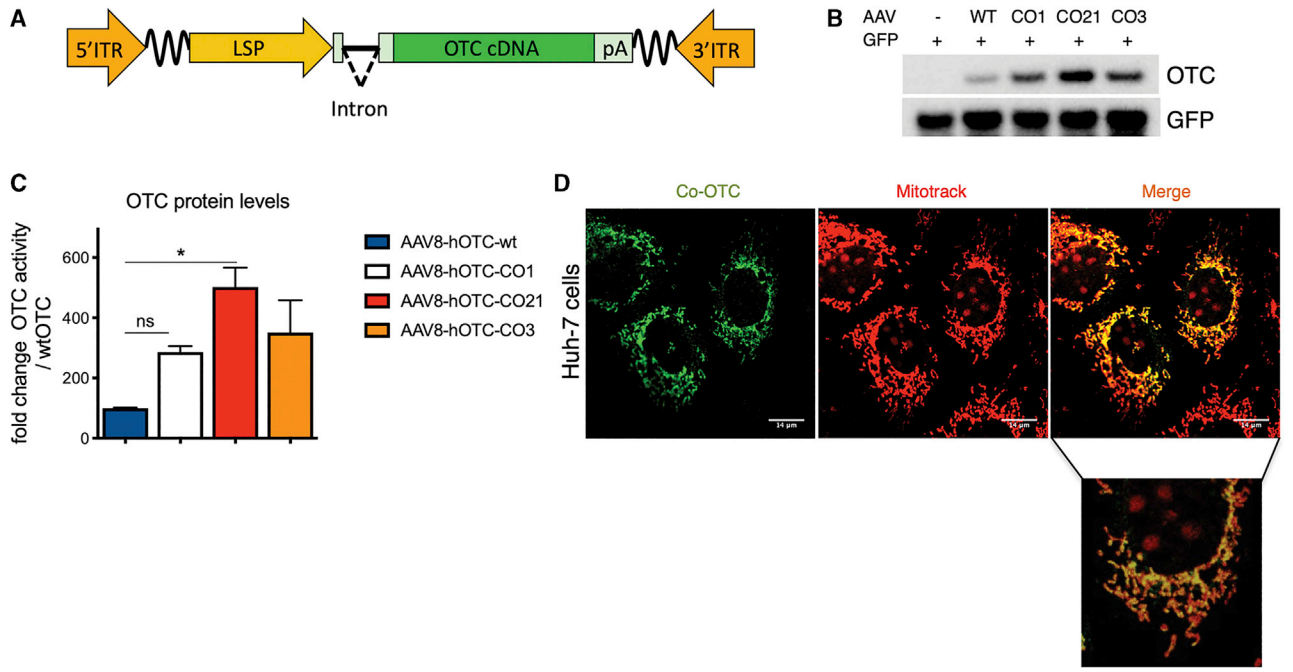

Figure 1. Codon optimization of the hOTC cDNA increases protein production without affecting sub-cellular localization

(A) Scheme of the rAAV-hOTC expression cassette. ITR, AAV2 inverted terminal repeat; intron, modified hemoglobin (*HBB2*) beta intron; LSP, liver-specific promoter (*ApoE*/h*AAT*, hybrid promoter containing *ApoE* enhancer and h*AAT* promoter); h*OTC*, WT or CO h*OTC* open reading frame (ORF); pA, hemoglobin beta (*HBB*) polyadenylation signal; the wavy lines indicate AAV backbone sequences between the expression cassette and ITRs. (B) Analysis of HCC cell line Huh-7 transfected with first group of hOTC-CO constructs. Representative western blot analysis of OTC protein levels in Huh-7 cell lysates (15 μg of protein per lane) following co-transfection of the pSMD2-hOTC-WT, pSMD2-hOTC-CO01, pSMD2-hOTC-CO21, and pSMD2-hOTC-CO03 constructs and GPF plasmids. The control lane contains cell lysate from cells transfected with the GFP-expressing plasmid. (C) Densitometric quantification of hOTC proteins from (B). GFP was used as transfection control. Values are expressed as fold change with respect to the pSMD2-hOTC-WT plasmid. Data are shown as mean ± SEM, and statistical analyses were performed by one-way ANOVA with Turkey's multiple comparison test (n = 2, *p < 0,05). (D) Sub-cellular localization studies of hOTC in Huh-7 human liver cells. Huh-7 cells were transfected with plasmids encoding the hOTC-CO21 variant. Mitochondria (red, MITO-TRACK) and hOTC (green) were detected with a confocal microscope. A magnified picture of the indicated area is shown below the low-resolution picture. The scale bar corresponds to 14 μm.

carcinomas (HCCs).[20] These sequences, located next to the AAV inverted terminal repeat (ITR) regions, contained transcription factor binding sites (TFBSs) that function as a liver-specific enhancer-promoter elements, potentially able to transactivate neighboring genes upon integration in the genome.[24] These observations highlight the importance of vector optimization and long-term safety assessments both in the preclinical and the clinical settings.

In the present work, we developed a therapeutic liver-specific AAV2/8 vector expressing a codon-optimized version of human *OTC* cDNA under the transcriptional control of the human alpha-1 antitrypsin (h*AAT*) promoter and apolipoprotein E (*ApoE*) enhancer[25], which was highly efficient in expressing an enzymatically active OTC protein, with long-term efficacy in rescuing the diseased phenotype of OTC$^{Spf\text{-}Ash}$ mice. In contrast to standard approaches,[18,26] we performed multiple rounds of codon-optimization of the human *OTC* (h*OTC*) cDNA via common algorithms and ortholog sequence analysis to improve mRNA translatability and therapeutic efficacy. This translationally optimized candidate clinical vector, in which the ITR-associated enhancer-promoter elements were removed, presents improved safety features, provides sustained therapeutic efficacy in OTC$^{Spf\text{-}Ash}$ mice, and therefore has the potential to achieve therapeutic efficacy in OTCD patients.

RESULTS

Codon optimization of human OTC significantly improves *in vitro* hOTC expression and activity

In order to improve the overall efficacy of the gene-therapy approach for OTCD, an initial set of codon-optimized (CO) variants of the *OTC* cDNA were generated using different optimization algorithms (CO3, CO9, CO6A, CO9-1, and CO9-2). The obtained sequences were then analyzed for the presence of potential cryptic splicing sites using splicing-specific software, which were manually removed. Potential alternative reading frames (ARFs) located in the coding and non-coding strands were also manually removed to decrease the risk of undesired cytotoxic T lymphocyte (CTL)-mediated immune responses directed against AAV-transduced hepatocytes expressing aberrant transgene products generated by ARFs, with the consequent reduction of overall efficacy.[25,27] The human WT h*OTC* cDNA and all different optimized h*OTC* cDNAs were cloned in the pSDMD2 vector, under the transcriptional control of the h*AAT* promoter and *ApoE* enhancer[25]

(liver-specific promoter [LSP]; Figure 1A). In addition, we synthesized the CO LW4 hOTC clinical candidate described by Wang et al.[18] and also cloned it into the pSDMD2 vector under the hAAT promoter (hOTC CO1 construct).

The resulting plasmids were transfected into the human liver cell line Huh-7 to evaluate the OTC protein expression levels (Figure 1B; Figures S1A and S1B). Western blot analysis demonstrated a variable range of protein levels, with some hOTC-CO variants showing a robust increase in the efficiency of protein production compared to the construct expressing the WT hOTC cDNA (Figures S1A and S1B; hOTC-CO1, hOTC-CO3, and hOTC-CO9).

In a second phase, we aligned the OTC amino acid sequences of 142 species (Figure S2; Table S1) to identify the conserved regions and domains containing the active site of the enzyme.[28,29] The alignments were manually adjusted to the human OTC primary sequence. Next, we generated additional *OTC* variants, hOTC-CO18 and hOTC-CO21, by shuffling the conserved domains (Figure S3) of the most active variants (hOTC-CO1, hOTC-CO3, and hOTC-CO9) from the initial phase of screening. After transient transfection in Huh-7 cells, we observed that the hOTC-CO21 version showed a 5-fold increase in protein expression levels, which was higher than the levels obtained with the original CO versions (Figures 1B and 1C; Figures S1A and S1B).

Importantly, we confirmed the correct mitochondrial import and subcellular localization of the hOTC proteins by assessing the co-localization of the exogenous hOTC proteins with the mitochondrial marker Mitotrack. As expected, all variants presented mitochondrial localization (Figure 1D; Figure S1C).

These results indicate that a combination of codon optimization and shuffling of conserved and active domain sequences is an effective strategy to derive highly expressed hOTC cDNA variants.

Codon optimization of human *OTC* cDNA significantly improves *in vivo* hOTC expression and activity

To further confirm the activity of these variants *in vivo*, AAV8-hOTC-WT, AAV8-hOTC-CO1, AAV8-hOTC-CO3, and AAV8-hOTC-CO21 were intravenously injected in adult WT mice at a dose of 5.0E12 viral genomes (vg)/kg. In line with the *in vitro* observations, hepatic expression levels and enzymatic activity were significantly increased upon treatment with the hOTC-CO1, hOTC-CO3, and hOTC-CO21 variants, compared to the hOTC-WT construct (Figures 2A–2C). Consistently, mice injected with hOTC-CO21 variant displayed a 5- to 6-fold increase in protein expression and enzyme activity compared to hOTC-WT and was significantly higher than that obtained with hOTC-CO1 and hOTC-CO3 (Figures 2A–2C). All injected animals had similar vg copy numbers (Figure 2D), suggesting that the observed differences in OTC protein levels and catalytic activity were related to the effect of different codon-optimization strategies on mRNA translation. Thus, based on *in vitro* and *in vivo* data, the variant hOTC-CO21 was identified as the most efficient one, compared to WT and CO1 hOTC cDNAs (Figures 1B, 1C, 2A, and 2D).

Interestingly, despite having a similar expected molecular weight (MW) (39.70 kDa and 39.87 kDa, for the human and mouse OTC, respectively) and 97.73% amino acid similarity, the human OTC protein migrated slower than the mouse counterpart (Figure S4).

These findings show that the CO AAV8-hOTC-CO21 vector was the most effective in robustly driving expression of the hOTC transgene *in vivo*.

AAV8-hOTC CO21-mediated gene therapy restores OTC expression and urea cycle in adult OTC$^{Spf\text{-}Ash}$ mice

To determine the therapeutic efficacy of AAV8-hOTC-CO21, we first performed a short-term dose-finding experiment in the OTC$^{Spf\text{-}Ash}$ mouse model of OTCD.[30,31]

AAV8-hOTC-WT and AAV8-hOTC-CO21 were injected in 12-week-old OTC$^{Spf\text{-}Ash}$ male mice with 3 different doses: 2.5E11, 5.0E11, and 1.0E12 vg/kg. Animals were sacrificed 8 weeks after AAV delivery. The therapeutic efficacy was determined by the correction of urinary orotic acid levels, the main biomarker for OTCD. The AAV8-hOTC-WT vector restored physiological levels of urinary orotic acid at the dose of 1.0E12 vg/kg but did not correct the phenotype at lower doses (Figure 3A). In contrast, the AAV8-hOTC-CO21 vector normalized urinary orotic acid in OTC$^{Spf\text{-}Ash}$ mice at a lower dose (5.0E11 vg/kg) compared to the human WT version (Figures 3A and 3B). Quantification of OTC protein in the liver by western blot analysis correlated with the observed therapeutic efficacy. The levels of OTC protein of WT animals were comparable to those obtained with the highest dose of the AAV8-hOTC-WT vector (1.0E12vg/kg), while in the case of the CO21 cDNA-expressing vector, the WT levels were comparable to those of the intermediate dose (5.0E11vg/kg) (Figures 3C–3F).

To note, the AAV8-hOTC-CO21 vector was able to restore WT levels of catalytically active OTC in the liver at a dose of 5.0E11 vg/kg (Figures 3G and 3H), with an ~20-fold increase in OTC enzyme activity compared to untreated OTC$^{Spf\text{-}Ash}$ mice (Figure 3G).

These data show that treatment of adult OTC$^{Spf\text{-}Ash}$ mice with AAV8-OTC-CO21 at a vector dose of 5.0E11 vg/kg was sufficient to express WT levels of human OTC and correct the phenotype in the short term and that the use of hOTC-CO21 CO transgene may allow for a 2-fold reduction of the therapeutic dose compared to the hOTC WT version.

Next, we assessed the ability of our therapeutic vector to restore the urea cycle in OTC$^{Spf\text{-}Ash}$ mice in an acute response to an ammonia challenge, a test commonly used to assess the clinical protection of the gene-therapy treatment against a provocative nitrogen acute increase.[15,17,32,33] A new group of adult OTC$^{Spf\text{-}Ash}$ mice was dosed with 5.0E11 vg/kg of AAV8-hOTC-WT or AAV8-hOTC-CO21

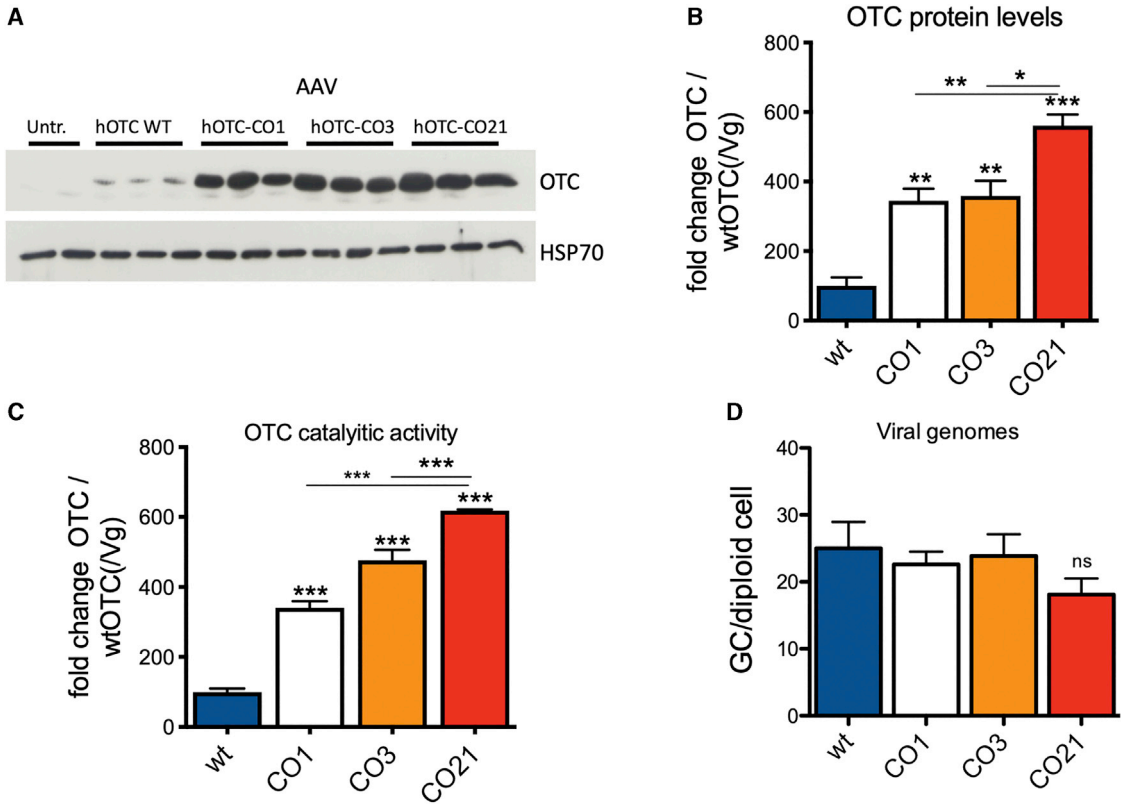

Figure 2. Analysis of WT male mice transduced with the AAV8 hOTC constructs

WT C57BL/6 male mice (8 weeks old) were i.v. transduced with 5.0E12 vg/kg of the indicated AAV2/8 constructs. Liver samples were collected at 14 days after viral transduction. (A) Representative WB analysis of liver extracts from control and AAV-treated animals (n = 3 per construct). Samples from two untreated mice were loaded in the first two lines of the gel. The OTC and HSP70 bands are shown. In the OTC panel, the faint band presenting a slightly faster mobility than the most prominent one corresponds to the endogenous murine OTC (see Figure S4). (B) Densitometric quantification of the Western blot (WB) of (A), relative to the OTC-WT values, normalized by the vg copy number (n = 3 per group). (C) OTC enzyme activity expressed in μmol of citrulline produced in 30 min of reaction, normalized by the vg copy number (n = 3 per group). (D) Viral genome copy number quantification by quantitative real-time PCR. The mean value of two independent determinations is indicated (n = 3 per group). Statistical significance compared to hOTC-WT is shown above the bar for each experimental group, and statistical significance between experimental groups is indicated by the horizontal line. (B) One-way ANOVA, $p < 0.0001$; (C) one-way ANOVA, $p < 0.0001$; (D) one-way ANOVA, not significant (NS); Tukey's comp. tests, $^{*}p < 0.05$, $^{**}p < 0.01$; $^{***}p < 0.001$.

(intravenously [i.v.]), and the ammonia challenge (7.5 mmol of ammonia/kg, intraperitoneally [i.p.]) was performed 4 and 8 weeks after vector dosing (Figure 4A). The efficiency of ammonia clearance was quantified 20 min after the challenge by determining plasma ammonia levels and scoring the animals for ataxia and gait abnormalities, seizures, and sound sensitivity (Figure 4B), as previously described.[15,17,32,33] The composite score of AAV8-hOTC-CO21-injected animals was comparable to that of untreated WT animals and AAV8-hOTC-WT-treated OTC$^{Spf\text{-}Ash}$ mice (Figure 4B). As expected, untreated OTC$^{Spf\text{-}Ash}$ mice were moribund and displayed a low behavioral score at the 4- and 8-week time points, with increased plasma ammonia levels, as a consequence of urea cycle dysfunction (Figures 4B and 4C). Treatment with either the AAV8-hOTC-WT or the AAV8-hOTC-CO21 vector successfully restored ammonia detoxification by reducing serum ammonia to physiological levels, after challenge with ammonia at both 4 weeks and 8 weeks post-gene-therapy injection (Figure 4C). These findings showed that an acute increase of ammonia in OTCD adult mice could be managed by AAV8-hOTC-CO21 vector-driven OTC hepatic expression. Enzyme catalytic activity was much higher with the AAV8-hOTC-CO21 vector as compared to AAV8-hOTC-WT construct (Figure 4D), confirming previous results obtained with a separate group of OTC$^{Spf\text{-}Ash}$ animals (Figure 3G).

Deletion of the HCC-related liver-specific enhancer sequence in the AAV backbone did not affect the therapeutic efficacy

In an effort to improve the potential safety of the gene-therapy vector, a variant of the AAV-hOTC-CO21 vector was generated in which putative liver-specific TFBSs, which may function as a liver-specific enhancer-promoters,[24] were removed (AAV-hOTC-CO21ΔEnhancer; Figure 5A) and tested side-by-side with the unmodified AAV-hOTC-CO21 vector at a dose of 1.0E12 vg/kg injected i.v. in adult OTC$^{Spf\text{-}Ash}$ mice. Urinary orotic acid levels were assessed every 2 weeks, and protein expression levels and vg copies were determined at sacrifice of the animals, 8 weeks after viral delivery (Figures 5B–5E). Treatment with either AAV-hOTC-CO21 or

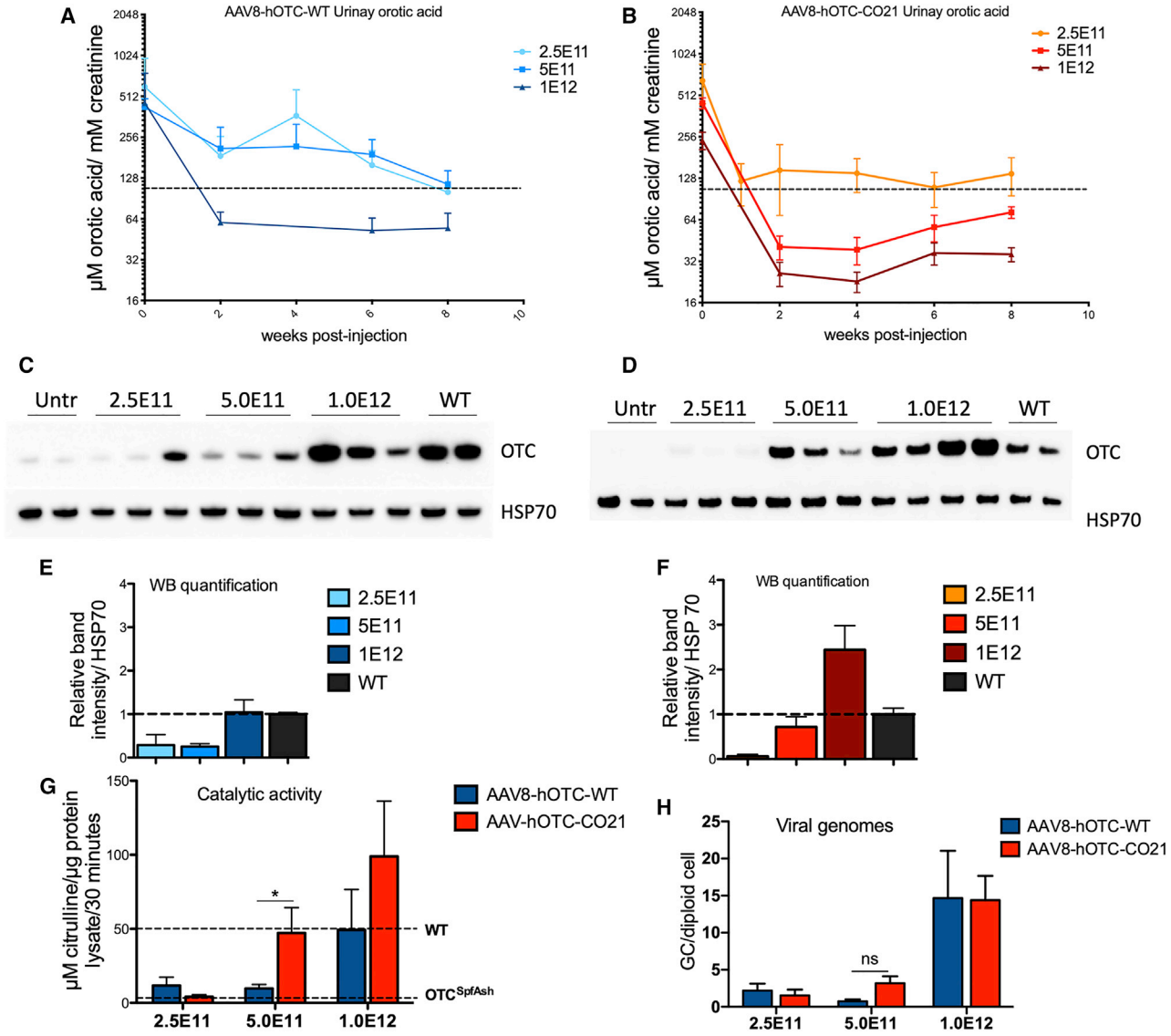

Figure 3. Side-by-side comparison in male OTC$^{Spf\text{-}Ash}$ mice transduced with AAV8-hOTC-WT and AAV8-hOTC-CO21

(A and B) 3-month-old OTC$^{Spf\text{-}Ash}$ mice were i.v. injected with 2.5E11 vg/kg (n = 4), 5.0E11 vg/kg (n = 5), or 1.0E12 vg/kg (n = 5) of AAV8-hOTC-WT (A) or AAV8-hOTC-CO21 (B). Mice were sacrificed 8 weeks after viral delivery. Urine samples were collected every 2 weeks post-injection and analyzed for orotic acid. The dashed line delimits the physiological level of orotic acid in WT animals. Two-way ANOVA, 5.0E11 vg/kg, AAV8-hOTC-WT versus AAV8-hOTC-CO21, $p < 0.01$. (C–F) OTC protein levels were determined by WB from liver extracts from AAV8-hOTC-WT (C) and AAV8-hOTC-CO21 (D). The densitometric quantification of the OTC-specific bands, normalized by the housekeeping HSP70 protein and vg copies is shown in (E) and (F). (G) OTC enzyme activity expressed in µmol of citrulline produced in 30 min of reaction. Enzyme activity of WT and OTC$^{Spf\text{-}Ash}$ liver extracts is indicated by the dashed lines. Data are shown as mean ± SEM, and statistical analyses were performed by one-way ANOVA with Turkey's multiple comparison test (n = 3–5 per group; *$p < 0.05$). (H) The vg particles were determined by quantitative real-time PCR, and the mean values of two independent determinations are indicated (n = 4–5 per group). Data are shown as mean ± SEM, and statistical analyses were performed by two-way ANOVA with Tukey's multiple comparison test (*$p < 0.05$).

AAV-hOTC-CO21ΔEnhancer vectors significantly decreased urinary orotic acid to normal levels, while no differences were observed between the treated groups (Figure 5B), which presented similar OTC protein levels and vg copy numbers in the liver (Figures 5C–5E). These findings indicate that the absence of the enhancer element had no significant impact in the activity of the *ApoE* enhancer and h*AAT* promoter, which drive transcription of the h*OTC* cDNA. Thus, for the next series of experiments, we utilized the AAV-hOTC-CO21ΔEnhancer vector.

AAV-hOTC-CO21ΔAV-hOTC vector drives long-term therapeutic efficacy in the mature liver

To assess the long-term therapeutic efficacy of gene transfer in adult mice, we treated 12-week-old OTC$^{Spf\text{-}Ash}$ mice with 5.0E11 or 1.0E12

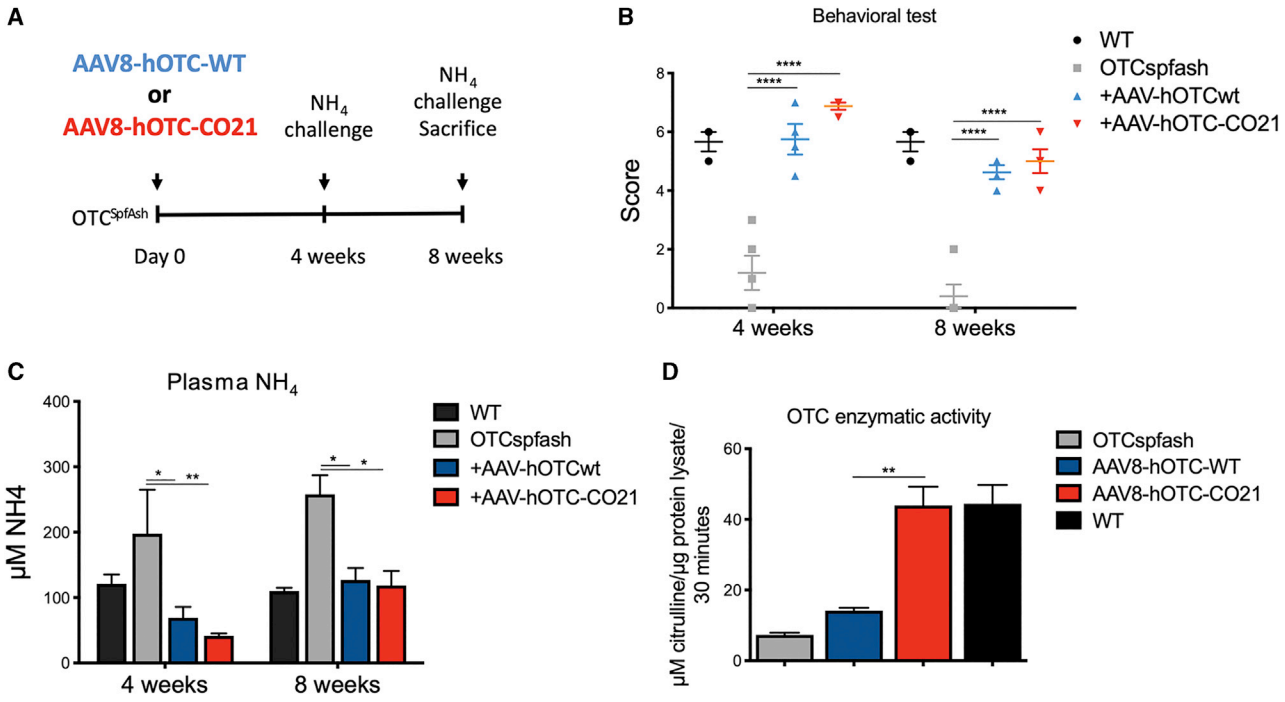

Figure 4. Ammonia challenge of OTC$^{Spf\text{-}Ash}$ mice injected with 5.0E11 vg/kg of AAV8-hOTC-WT and AAV8-hOTC-CO21

(A) Experimental scheme. 12-week-old mice were i.v. injected with 5.0E11 vg/kg of the indicated AAV8 constructs (n = 4). (B–D) Ammonia challenge was performed twice: at 4 and at 8 weeks post-injection. In each challenge, mice were evaluated with a set of behavioral tests (B), and plasma ammonia levels were determined (C). At 8 weeks post-injection, mice were sacrificed and liver was analyzed for OTC catalytic activity (D). Data are shown as mean ± SEM, and statistical analyses were performed by two-way ANOVA with Bonferroni's multiple comparison test (*p < 0.05; **p < 0,01; ***p < 0.001).

vg/kg of AAV-hOTC-CO21ΔEnhancer vector and animals were followed up for 40 weeks. Urinary orotic acid levels were monitored for the duration of the experiment, while genome copy number and OTC enzymatic activity and protein levels were determined in the liver at the sacrifice (Figure 6). In line with previous experiments, both groups of animals presented stable urinary orotic acid levels, which were within normal values for the whole duration of the experiment. As expected, we observed lower urinary orotic acid levels in the animals treated with the higher vector dose (Figure 6A). A dose effect was observed for OTC protein levels, enzymatic activity, and vg copies measured in the liver (Figures 6B–6E). These results indicate that our AAV-hOTC-CO21ΔEnhancer vector provided efficient and durable correction of OTC expression and activity in adult mice.

A high dose of AAV-hOTC-CO21 vector does not increase serum levels of liver transaminase

To get a deeper insight on the safety of the procedure, we injected OTC$^{Spf\text{-}Ash}$ mice with a dose that was 13 times higher than the therapeutic dose determined in the previous experiments (1.3E13 vg/kg), a dose similar to the high vector dose used in a current clinical trial for OTCD (ClinicalTrials.gov: NCT02991144). Urinary orotic acid and liver transaminases (aspartate aminotransferase, AST, and alanine aminotransferase, ALT) were determined at 2, 7, and 14 days after treatment. Urinary orotic acid levels were below the normal values, while no increases over normal levels were observed in serum liver transaminases, with values similar to those of untreated mice (Figure S5).

These results provide preliminary insights on the safety and efficacy of the AAV-hOTC-CO21ΔEnhancer vector and support the potential translation of the therapeutic approach to OTCD patients.

DISCUSSION

Liver gene therapy in hemophilia A and B clinical trials have shown safety and therapeutic potential of AAV vectors.[11–14] However, a metabolic disease such as OTCD presents a more challenging clinical condition for gene-replacement therapy, due to the severity of the disease. Potentially lethal hyperammonaemic episodes must be prevented in all severely affected male pediatric patients since birth, some of which are awaiting liver transplantation. In addition, about 20% of adult heterozygous females present with clinical manifestations.[5] The higher severity of OTCD, compared to hemophilia A and B, which require lower production of the therapeutic protein,[11–14] suggests that normalization of hepatic expression of OTC mediated by gene therapy may require efficient transduction of hepatocytes and elevated levels of the enzyme activity and, consequently, a highly effective gene-replacement vector.

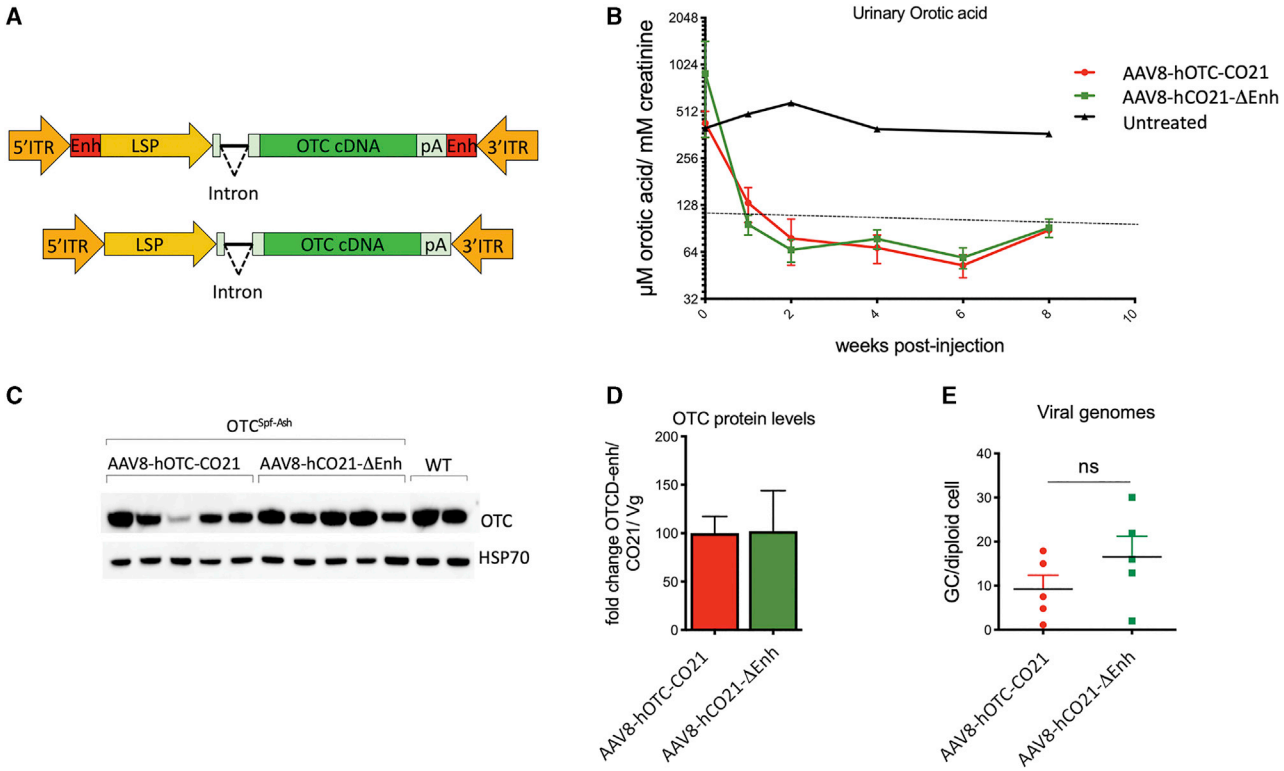

Figure 5. Deletion of liver-specific enhancer sequences in the AAV vector backbone does not affect therapeutic efficacy

(A) The segments next to the AAV ITRs containing liver-specific transcription binding sites (Enh, indicated as red rectangles) were removed to generate the AAV8-hOTC-CO21ΔEnh vector (bottom). ITR, AAV2 inverted terminal repeat; intron, modified hemoglobin (*HBB2*) beta intron; LSP, liver-specific promoter (*ApoE*/h*AAT*, hybrid promoter containing *ApoE* enhancer and h*AAT* promoter); hOTC, WT or CO hOTC open reading frame (ORF); pA, hemoglobin beta (*HBB*) polyadenylation signal. (B) 3-month-old $OTC^{Spf\text{-}Ash}$ mice were i.v. injected with 5.0E11 vg/kg of AAV8-hOTC-CO21 or AAV8-hOTC-CO21ΔEnh (n = 5 per group). Animals were sacrificed 8 weeks after viral delivery. Urine samples were collected every 2 weeks post-injection and analyzed for orotic acid levels. Orotic acid values were standardized against creatinine levels. Dashed line delimits physiological level of orotic acid. (C) OTC protein levels were determined by WB analysis. (D) Densitometric quantification of the WB of (C), normalized by the vg copy number. Data are shown as mean ± SEM. (E) The vg particles were determined by quantitative real-time PCR, and the mean values of two independent determinations are indicated. Data are shown as mean ± SEM, and statistical analyses were performed by unpaired *t* test (*$p < 0.05$).

To generate a highly expressed hOTC cDNA we used a combined strategy: initially, a series of CO *OTC* cDNAs were generated using different codon-optimization algorithms and evaluated for expression *in vitro* and *in vivo*. Next, the conserved domains and active sites of the most active constructs were shuffled to achieve an optimally expressed sequence, without altering the native amino acid sequence of the human enzyme. The conserved regions were identified by performing an alignment of OTC amino acid sequences of 142 species (Figure S2).[28,29] The shuffling of the conserved regions of the CO sequences generated an *OTC* cDNA, hOTC-CO21, that outperformed all previously tested hOTC CO versions. The optimized AAV8-hOTC-CO21 vector provided protein production and enzymatic activity up to 5- to 6-fold higher compared to those obtained with the WT hOTC cDNA, in both *in vitro* and *in vivo* experiments.

Using conventional algorithms, Wang et al.[18] also reported highly expressed CO hOTC cDNA versions under the control of the thyroxine-binding globulin (*TBG*) gene promoter. We created a construct, hOTC-CO1, with the CO sequence described by Wang et al.[18] using the same promoter and other cassette elements as those used in AAV-hOTC-CO21. A side-by-side analysis showed increased protein production and enzymatic activity in the animals treated with the AAV vector expressing the hOTC-CO21 cDNA, compared to those expressing the hOTC-CO1 cDNA.

The AAV8-hOTC-CO21ΔEnhancer gene-therapy vector presented here allowed the complete and long-term correction of the phenotype present in $OTC^{Spf\text{-}Ash}$ mice at a relatively low dose. Our data demonstrated that the 5.0E11 vg/kg dose was able to robustly restore WT levels of liver OTC expression and activity, normalizing urinary orotic acid levels, the main biomarker of OTCD.[6] Importantly, this dose completely restored the urea cycle, with normalization of behavioral parameters and clinical protection during an acute ammonia challenge, similar to those observed in WT animals. This test has particular relevance, since a bolus of ammonia, the main neurotoxic metabolite that accumulates upon dysfunction of the urea cycle,[34] is given to the animals, and the OTC absence or its reduced activity results in immediate serious dysfunctions

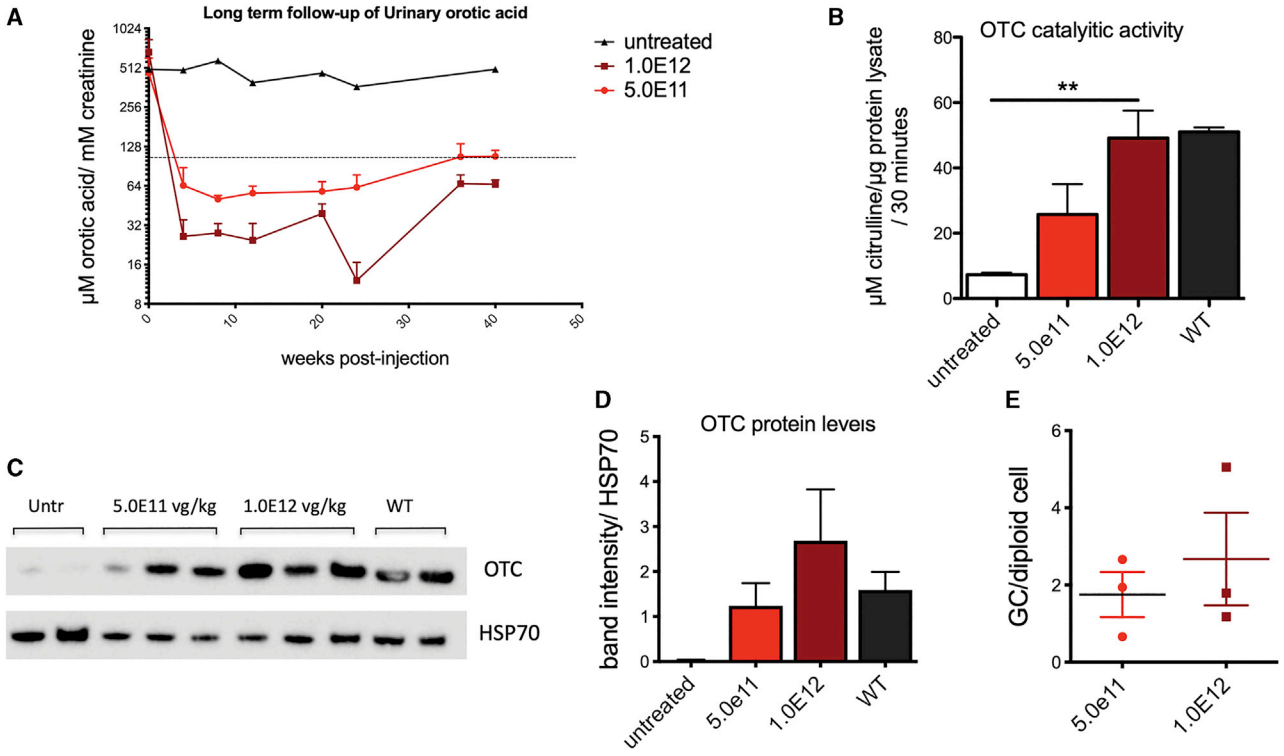

Figure 6. Long-term evaluation of hOTC-CO21 transgene expression in adult OTC$^{Spf\text{-}Ash}$ mice

12-week-old mice were i.v. injected with 5.0E11 vg/kg or 1.0E12 vg/kg of the AAV8-hOTC-CO21 or AAV8-hOTC-CO21ΔEnh constructs (n = 4). Animals were sacrificed 40 weeks after viral delivery. (A) Urine samples were collected every 2 weeks post-injection and analyzed for orotic acid levels. Orotic acid values were standardized against creatinine levels. Dashed line delimits physiological level of orotic acid. (B) OTC enzyme activity expressed in µmol of citrulline produced in 30 min of reaction. Data are shown as mean ± SEM, and statistical analyses were performed by one-way ANOVA with Turkey's multiple comparison test (**$p < 0.05$). (C) OTC protein levels were determined by WB analysis. HSP70 was used to normalize for protein load. Untr, untreated OTC^{SpfAsh} mice. (D) Densitometric quantification of the WB of (C). WT, untreated wild-type control animals. Data are shown as mean ± SEM, and statistical analyses were performed by one-way ANOVA with Turkey's multiple comparison test. (E) The vg particles were determined by quantitative real-time PCR, and the mean values of two independent determinations are indicated. Data are shown as mean ± SEM, and statistical analyses were performed by unpaired t test. (*$p < 0.05$).

or death.[18,33] Importantly, the improvements in the therapeutic vector described here would allow for an important decrease in the therapeutic dose, thus reducing its genotoxic potential[19] and, consequently, increasing the overall safety of the approach. OTC expression levels correlated with catalytic activity, suggesting that the expressed exogenous protein was fully active in the hepatocytes. Moreover, we verified the correct subcellular localization of the OTC protein produced by the therapeutic vector, demonstrating that it is efficiently processed and translocated to mitochondria.

One of the potential safety concerns is genotoxicity of the AAV vector. In spite of being episomal vectors, preclinical studies have shown that a minor proportion of the viral AAV genomes may be randomly inserted into the host genome[35,36] with the risk of insertional mutagenesis and transactivation of nearby genes.[21,22,37] Factors such as the total vector dose and the promoter choice may affect the genotoxicity risk of AAV vectors.[19] In effect, the presence of the chicken β-actin (*CBA*) promoter or the liver-specific *TBG* promoter, commonly used in AAV vectors, results in the development of HCC when delivered in neonate mice at doses of 1–2E11 vg/pup. Here, we have endeavored to minimize the genotoxicity potential of the therapeutic vector by selecting the h*AAT* promoter containing the *ApoE* enhancer,[25] which was not associated with hepatocellular cancers,[19] and a CO transgene sequence that allows for lower doses of vector. Additionally, sequences flanking the WT AAV ITRs have been found integrated in known cancer driver genes in patients with HCC.[20] Importantly, preclinical studies suggest that these sequences contain liver-specific TFBSs, promoting transcription of nearby genes,[24] with the risk of tumorigenesis.[20–22,37] Thus, to further mitigate the potential risk of hepatocarcinogenicity, we removed these transcriptional activator regions present in the AAV backbone. Deletion of these sequences did not affect gene expression and the therapeutic potential of our vector, suggesting that their role in transcription is dispensable in the presence of a strong LSP. Importantly, treatment with the AAV8-hOTC-CO21ΔEnhancer gene therapy did not result in liver damage or tumorigenesis, although further experimentation at higher vector doses and longer time may be needed to conclusively show the improved vector safety properties.

Thus, the results presented here further support the safe use of the AAV8-hOTC-CO21ΔEnhancer gene-therapy vector in clinical trials of OTCD patients. A clinical trial of AAV gene transfer for OTCD is currently ongoing (ClinicalTrials.gov: NCT02991144). While results are not published, early data emerging from the study indicate that high vector doses (1.0E13 vg/kg) are needed to achieve full therapeutic efficacy, which are associated with increase in liver enzymes and require the use of prophylactic immunomodulation (https://ir.ultragenyx.com/news-releases/news-release-details/ultragenyx-announces-positive-longer-term-results-first-three). Thus, the development of highly optimized gene transfer vectors could reduce the therapeutic vector dose and help mitigate potential vector genotoxicity and immune-mediated toxicities in humans (reviewed in Verdera et al.[38]).

An appropriate timing for the application of gene therapy is crucial for reasons related to the characteristics of both the disease and the vector. OTCD may present acutely soon after birth, during childhood, or in adulthood. In the neonatal-onset form of OTCD, the liver suffers from an acute toxic injury resulting in liver necrosis and regeneration, a condition that may be unsuitable for effective episomal gene transfer with non-integrative vectors. The infantile-onset form of OTCD represents a larger cohort of severely affected patients with normal liver architecture and function and are potential candidates for AAV gene therapy.[39] However, the therapeutic approach may still require further improvements to be applied in the neonatal/infantile setting. In fact, gene therapy in this context will probably result in the gradual loss of AAV DNA during hepatocyte duplication and, consequently, loss of therapeutic efficacy during liver growth,[16,40–42] requiring re-administration of the therapeutic medical product. Currently, vector re-dosing is limited by the generation of high-titer anti-AAV neutralizing antibodies (Nab) that may block vector transduction.[11,43–45] Thus, novel approaches should be developed to allow AAV re-administration in this challenging disease. Different strategies are being studied, such as interfering with the immune response at the time of viral administration[46–48] or depleting the serum of the patient from Nab generated during the first AAV administration.[49–51] Recently, co-administration of AAV8 vectors with ImmTOR nanoparticles containing rapamycin have been shown to mitigate the formation of anti-AAV antibodies and enable vector re-dosing in mice and non-human primates.[48] However, these promising approaches still require validation in the clinic.

In conclusion, considering that safety and efficacy are main requirements of vector development, in this study we developed an efficient and safe therapeutic vector able to completely rescue the phenotype of adult OTC-deficient Spf-Ash mice at relatively low AAV doses. Long-term follow-up of treated animals demonstrated steady expression of hOTC in the mouse liver with complete normalization of the disease phenotype, supporting the potential translation of this gene-transfer strategy to patients affected by OTCD.

MATERIALS AND METHODS

AAV vector construction

The h*OTC* cDNA was inserted in the pSDMD rAAV vector previously described.[25] Transcription of the h*OTC* transgene was driven by a hybrid promoter containing the *ApoE* enhancer and the *hAAT* promoter and terminated by the hemoglobin beta (*HBB*) polyadenylation signal. The coding region and the promoter are separated by a human hemoglobin beta-derived synthetic intron (*HBB2*) modified by removal of alternative open reading frames longer than 50 base pairs.[25] CO variants of the *OTC* cDNA were generated using different optimization algorithms (Genscript, IDT, JCat, GeneArt, DNA 2.0) and cloned into the pSDMD rAAV vector. DNA synthesis was performed by Genscript, USA. The potential cryptic splicing sites were detected using a splicing-specific software and were manually removed. Potential alternative ARFs longer than 50 bases located in the coding and non-coding strands were manually removed. The hOTC-CO18 and hOTC-CO21 cDNA variants were generated by shuffling the conserved regions and domains containing the active sites of the most active versions. The conserved regions were identified by the alignment of OTCases of 142 species. OTC sequences from a broad range of species from bacteria to human were obtained from the Uniprot databank (Table S1), aligned, and analyzed for sequence conservation using the Seq2Logo software (http://www.cbs.dtu.dk/biotools/Seq2Logo/). The AAV-hOTC-CO21ΔEnhancer vector is devoid of 2 sequences containing enhancing elements downstream of the 5' ITR (5'gtagttaatgattaacccgccatgctacttatctacg tagccatgct 3') and upstream of the 3' ITR (5'agcatggctacgtagataagtag catggcgggttaatcattaactac 3').

AAV vector production

Research-grade AAV vectors pseudo-serotyped with the AAV8 capsid proteins were produced according to a modified version of the adenovirus-free transient transfection methods as previously described[52] and purified by CsCl gradient centrifugation.[53,54]

Genome-containing AAV vectors and empty AAV capsid particles were titrated using a quantitative real-time polymerase chain reaction and confirmed by SDS-PAGE followed by SYPRO Ruby protein gel stain and band densitometry.

Cell culture and transfection

Human Huh-7 cells were maintained in Dulbecco's modified 's medium (DMEM; Thermo Fisher Scientific, Gibco) supplemented with 10% fetal bovine serum and 1% antibiotic+antimycotic solution (Sigma-Aldrich). Huh-7 cells were transfected with AAV8-hOTC and pGFP-C2 plasmid using lipofectamine 2000 (Invitrogen) following the manufacturer's instructions.

OTC immunostaining in Huh-7 cells

24 h after transfection, Huh-7 cells were incubated with the Mitotracker red FM (Thermo Fisher) probe following manufacturer's instructions. After 30 min of incubation, cells were washed with PBS and fixed for 10 min in formaldehyde solution (4%). After 3 consecutive washes with PBS, cells were incubated in blocking buffer (5% normal goat serum, 0.3% Triton-X, PBS) for 1 h. Rabbit anti-human OTC antibody from Abcam (Ab203859) was incubated for 2 h (dilution 1/100), followed by 1 h incubation with the secondary antibody (Alexa Fluor 488 goat anti-rabbit A11034). Cells were then analyzed by confocal microscopy.

Mouse model and animal studies

All animal care and experimental procedures were evaluated and approved by the ICGEB board and the Italian Ministry of Health (Ministero Italiano della Salute, authorization no. 926/2017-PR), with the full respect to the EU directive 2010/63/EU.

Breeding pairs of $OTC^{Spf\text{-}Ash}$ mice (B6EiC3Sn a/A-$OTC^{Spf\text{-}Ash}$/J) were purchased from Jackson Laboratories (stock no. 001811), and the colony was expanded and maintained in the ICGEB Bio experimentation facility. All injections were administered via the i.v. (tail vein) route at 8–16 weeks of age in male hemizygote $OTC^{Spf\text{-}Ash}$ mice.

Western blot analysis

Cells were collected and lysed in lysis buffer (0.5% triton-X, 10 mM HEPES [pH 7.4], 2 mM DTT). 20 μg of total cellular lysates were separated on 4%–12% Bis-Tris NuPage gel (Invitrogen).

Livers were collected and reduced in powder using a mortar and liquid nitrogen. Total liver protein extracts were extracted with a homogenizer in lysis buffer. Proteins in total liver lysates (1 μg per lane for WT mouse lysates and 8 μg per lane for $OTC^{Spf\text{-}Ash}$ lysates) were separated on a 10% SDS gel or Precast 4%–10% SDS gel (Invitrogen).

Proteins were transferred onto a nitrocellulose membrane, blocked with Blok-CH reagent (Millipore), and probed with rabbit anti-human OTC antibody (Abcam, Ab203859; dilution 1/3,000) and anti-hsp70 antibody (dilution 1/8,000). The primary antibody was detected with a goat anti-rabbit immunoglobulin G-horseradish peroxidase (IgG-HRP) or anti-rat, respectively.

OTC enzyme activity assay

OTC enzyme activity was determined in total liver protein extracts as reported previously,[55] with minor modifications. 1 μg of total liver protein extract (in lysis buffer) was added to 350 μL of reaction mixture (5 mM ornithine, 15 mM carbamyl phosphate, and 270 mM triethanolamine [pH 7.7]) and incubated at 37°C for 30 min. The reaction was then stopped by adding 125 μL of 3:1 phosphoric/sulfuric acid solution followed by 25 μL of 3% 2,3-butanedione monoxime and incubated at 95°C for 15 min in the dark. Citrulline production was determined by measuring the absorbance at 490 nm. The assays were performed in duplicate.

Viral genome copy quantification in the liver

Genomic DNA was extracted from pulverized liver using the Wizard SV genomic DNA purification system (Promega) following the manufacturer's guidelines. Vector genomes in liver were quantified by real-time PCR using the iQ SYBER green supermix (Bio-Rad), using primers targeting inside the promoter region as previously described.[40]

Urinary orotic acid determination

Urine was freshly collected before treatment (T0) and every 2 weeks or every month after the treatment and analyzed for orotic acid by high-performance liquid chromatography (HPLC)-tandem mass spectrometry, as described below.

Orotic acid was purchased from Sigma-Aldrich. The isotopically labeled internal standard orotic acid was purchased from Cambridge Isotope Laboratories.

The quantitative experiments were done using as internal standard the isotopically labeled 1,3-15N2 orotic acid in 200 μM concentration both for calibration curve and samples.

A typical calibration curve ranged from 15 μM to 300 μM with excellent linearity ($R^2 > 0.99$). A Bruker (Bremen, Germany) amaZonSL bench-top ion trap mass spectrometer, equipped with an electrospray source, was employed for this study. The source was operated in negative-ion mode with a needle potential of 4,500 V and a gas flow of 12 L/min of nitrogen with heating at 200°C. The chromatographic separations for quantitative experiments were performed using a series 1260 Agilent Technologies (Waldbronn, Germany) HPLC with autosampler controlled from the Bruker Hystar data system. A Phenomenex (Torrance, USA) HPLC column Gemini C18 5 μm, 110Å, 2× 150-mm was employed. Column flow rate was 0.4 mL/min, and elution was performed using 5 min wash time after 10-μL injection and a 3 min gradient from water with 0.1% formic acid to 90% acetonitrile with 0.1% formic acid. The tandem mass spectrometry (MS/MS) transitions used for the quantitative experiments (multiple reaction monitoring, MRM) were m/z 155.1 to 111.1 (orotic acid) and 157.1 to 113.1 (1,3-15N2 orotic acid). The acquired data were processed using the Bruker Compass Data Analysis proprietary software.

Creatinine was measured using the mouse creatinine kit (Crystal Chem, 80350) following the manufacturer's guidelines and used to normalize orotic acid values in the urine.

Ammonia challenge

Ammonia challenge was performed on a dedicated group of mice at 4 and 8 weeks post-AAV treatment. After the second challenge, the mice were sacrificed and the livers were collected to analyze OTC enzymatic activity and vg. For the challenge, mice were injected intraperitoneally with a 0.75 M NH_4Cl solution at the dose of 7.5 mmol/kg. Twenty minutes after the injection, mice were subjected to a behavioral test as previously described.[15,17,32,33] As described, the score was based on ataxia, response to sound, and seizure, using a scale from 0 to 3, with 3 indicating normal and 0 indicating the most severe impairment. The genotype of the animals and the treatment were unknown to the operator. Untreated $OTC^{Spf\text{-}Ash}$ and WT littermates were used as controls. Immediately after the behavioral test, urine was collected to analyze orotic acid, and a blood sample was collected by cheek puncture to analyze ammonia using the ammonia kit (Sigma AA0100) following the manufacturer's instructions.

Transaminanse determination

Transaminases were determined in serum using the ALT activity assay (Sigma-Aldrich, cat. no. MAK052) and the AST activity assay (Sigma-Aldrich, cat. no. MAK055) kits, following the manufacturer's instructions.

Statistical analysis

Data are expressed as means ± SD or mean ± SEM, as indicated. Statistical analyses were performed with the GraphPad Prism package. Two-tailed unpaired Student's *t* test was performed to compare 2 groups; one-way ANOVA followed by the indicated post hoc tests were performed when comparing more than two groups. Two-way ANOVA followed by the indicated post hoc tests were performed when comparing more than two groups relative to two factors. A p value <0.05 was considered statistically significant.

SUPPLEMENTAL INFORMATION

Supplemental Information can be found online at https://doi.org/10.1016/j.omtm.2020.11.005.

ACKNOWLEDGMENTS

The authors thank the ICGEB BioExperimentation Facility for help with animal care. This work was supported by ICGEB intramural funding to AFM and by Selecta Biosciences.

AUTHOR CONTRIBUTIONS

A.F.M., T.K.K., P.I., L.D.A., and F.M. conceived the project and analyzed data; F.B., G.B., E.N., and P.I. analyzed data; G.D.S. performed most experiments and analyzed data; C.G. performed the orotic acid determination; A.I., F.C., G.R., M.S.S., P.V., J.R., and S.C. performed cloning and preparation of AAV stocks; A.F.M. and G.D.S. wrote the manuscript. All authors read and participated in the correction of the manuscript.

DECLARATION OF INTERESTS

F.M. is currently an employee of Spark Therapeutics, a Roche company. P.I. and T.K.K. are employees of Selecta Biosciences.

REFERENCES

1. Gordon, N. (2003). Ornithine transcarbamylase deficiency: a urea cycle defect. Eur. J. Paediatr. Neurol. *7*, 115–121.
2. Pampols, T. (2010). Inherited metabolic rare disease. Adv. Exp. Med. Biol. *686*, 397–431.
3. Applegarth, D.A., Toone, J.R., and Lowry, R.B. (2000). Incidence of inborn errors of metabolism in British Columbia, 1969-1996. Pediatrics *105*, e10.
4. Summar, M.L., Koelker, S., Freedenberg, D., Le Mons, C., Haberle, J., Lee, H.-S., and Kirmse, B.; European Registry and Network for Intoxication Type Metabolic Diseases (E-IMD). Electronic address: http://www.e-imd.org/en/index.phtml; Members of the Urea Cycle Disorders Consortium (UCDC). Electronic address: http://rarediseases-network.epi.usf.edu/ucdc/ (2013). The incidence of urea cycle disorders. Mol. Genet. Metab. *110*, 179–180.
5. Brusilow, S.W., and Maestri, N.E. (1996). Urea cycle disorders: diagnosis, pathophysiology, and therapy. Adv. Pediatr. *43*, 127–170.
6. Häberle, J., Boddaert, N., Burlina, A., Chakrapani, A., Dixon, M., Huemer, M., Karall, D., Martinelli, D., Crespo, P.S., Santer, R., et al. (2012). Suggested guidelines for the diagnosis and management of urea cycle disorders. Orphanet J. Rare Dis. *7*, 32.
7. Enns, G.M., Berry, S.A., Berry, G.T., Rhead, W.J., Brusilow, S.W., and Hamosh, A. (2007). Survival after treatment with phenylacetate and benzoate for urea-cycle disorders. N. Engl. J. Med. *356*, 2282–2292.
8. Adam, R., Karam, V., Delvart, V., O'Grady, J., Mirza, D., Klempnauer, J., Castaing, D., Neuhaus, P., Jamieson, N., Salizzoni, M., et al.; All contributing centers (www.eltr.org); European Liver and Intestine Transplant Association (ELITA) (2012). Evolution of indications and results of liver transplantation in Europe. A report from the European Liver Transplant Registry (ELTR). J. Hepatol. *57*, 675–688.
9. Neuberger, J. (2016). An update on liver transplantation: A critical review. J. Autoimmun. *66*, 51–59.
10. Herrero, J.I. (2009). De novo malignancies following liver transplantation: impact and recommendations. Liver Transpl. *15* (*Suppl 2*), S90–S94.
11. Nathwani, A.C., Reiss, U.M., Tuddenham, E.G., Rosales, C., Chowdary, P., McIntosh, J., Della Peruta, M., Lheriteau, E., Patel, N., Raj, D., et al. (2014). Long-term safety and efficacy of factor IX gene therapy in hemophilia B. N. Engl. J. Med. *371*, 1994–2004.
12. Nathwani, A.C., Tuddenham, E.G., Rangarajan, S., Rosales, C., McIntosh, J., Linch, D.C., Chowdary, P., Riddell, A., Pie, A.J., Harrington, C., et al. (2011). Adenovirus-associated virus vector-mediated gene transfer in hemophilia B. N. Engl. J. Med. *365*, 2357–2365.
13. Rangarajan, S., Walsh, L., Lester, W., Perry, D., Madan, B., Laffan, M., Yu, H., Vettermann, C., Pierce, G.F., Wong, W.Y., and Pasi, K.J. (2017). AAV5-Factor VIII Gene Transfer in Severe Hemophilia A. N. Engl. J. Med. *377*, 2519–2530.
14. George, L.A., Sullivan, S.K., Giermasz, A., Rasko, J.E.J., Samelson-Jones, B.J., Ducore, J., Cuker, A., Sullivan, L.M., Majumdar, S., Teitel, J., et al. (2017). Hemophilia B Gene Therapy with a High-Specific-Activity Factor IX Variant. N. Engl. J. Med. *377*, 2215–2227.
15. Moscioni, D., Morizono, H., McCarter, R.J., Stern, A., Cabrera-Luque, J., Hoang, A., Sanmiguel, J., Wu, D., Bell, P., Gao, G.P., et al. (2006). Long-term correction of ammonia metabolism and prolonged survival in ornithine transcarbamylase-deficient mice following liver-directed treatment with adeno-associated viral vectors. Mol. Ther. *14*, 25–33.
16. Cunningham, S.C., Spinoulas, A., Carpenter, K.H., Wilcken, B., Kuchel, P.W., and Alexander, I.E. (2009). AAV2/8-mediated correction of OTC deficiency is robust in adult but not neonatal Spf(ash) mice. Mol. Ther. *17*, 1340–1346.
17. Wang, L., Wang, H., Morizono, H., Bell, P., Jones, D., Lin, J., McMenamin, D., Yu, H., Batshaw, M.L., and Wilson, J.M. (2012). Sustained correction of OTC deficiency in spf(ash) mice using optimized self-complementary AAV2/8 vectors. Gene Ther. *19*, 404–410.
18. Wang, L., Morizono, H., Lin, J., Bell, P., Jones, D., McMenamin, D., Yu, H., Batshaw, M.L., and Wilson, J.M. (2012). Preclinical evaluation of a clinical candidate AAV8 vector for ornithine transcarbamylase (OTC) deficiency reveals functional enzyme from each persisting vector genome. Mol. Genet. Metab. *105*, 203–211.
19. Chandler, R.J., LaFave, M.C., Varshney, G.K., Trivedi, N.S., Carrillo-Carrasco, N., Senac, J.S., Wu, W., Hoffmann, V., Elkahloun, A.G., Burgess, S.M., and Venditti, C.P. (2015). Vector design influences hepatic genotoxicity after adeno-associated virus gene therapy. J. Clin. Invest. *125*, 870–880.
20. Nault, J.-C., Mami, I., La Bella, T., Datta, S., Imbeaud, S., Franconi, A., Mallet, M., Couchy, G., Letouzé, E., Pilati, C., et al. (2016). Wild-type AAV Insertions in Hepatocellular Carcinoma Do Not Inform Debate Over Genotoxicity Risk of Vectorized AAV. Mol. Ther. *24*, 660–661.
21. Donsante, A., Miller, D.G., Li, Y., Vogler, C., Brunt, E.M., Russell, D.W., and Sands, M.S. (2007). AAV vector integration sites in mouse hepatocellular carcinoma. Science *317*, 477.
22. Donsante, A., Vogler, C., Muzyczka, N., Crawford, J.M., Barker, J., Flotte, T., Campbell-Thompson, M., Daly, T., and Sands, M.S. (2001). Observed incidence of tumorigenesis in long-term rodent studies of rAAV vectors. Gene Ther. *8*, 1343–1346.
23. La Bella, T., Imbeaud, S., Peneau, C., Mami, I., Datta, S., Bayard, Q., Caruso, S., Hirsch, T.Z., Calderaro, J., Morcrette, G., et al. (2020). Adeno-associated virus in the liver: natural history and consequences in tumour development. Gut *69*, 737–747.
24. Logan, G.J., Dane, A.P., Hallwirth, C.V., Smyth, C.M., Wilkie, E.E., Amaya, A.K., Zhu, E., Khandekar, N., Ginn, S.L., Liao, S.H.Y., et al. (2017). Identification of liver-specific enhancer-promoter activity in the 3′ untranslated region of the wild-type AAV2 genome. Nat. Genet. *49*, 1267–1273.
25. Ronzitti, G., Bortolussi, G., van Dijk, R., Collaud, F., Charles, S., Leborgne, C., Vidal, P., Martin, S., Gjata, B., Sola, M.S., et al. (2016). A translationally optimized AAV-UGT1A1 vector drives safe and long-lasting correction of Crigler-Najjar syndrome. Mol. Ther. Methods Clin. Dev. *3*, 16049.

26. Wang, L., Bell, P., Morizono, H., He, Z., Pumbo, E., Yu, H., White, J., Batshaw, M.L., and Wilson, J.M. (2017). AAV gene therapy corrects OTC deficiency and prevents liver fibrosis in aged OTC-knock out heterozygous mice. Mol. Genet. Metab. *120*, 299–305.

27. Li, C., Goudy, K., Hirsch, M., Asokan, A., Fan, Y., Alexander, J., Sun, J., Monahan, P., Seiber, D., Sidney, J., et al. (2009). Cellular immune response to cryptic epitopes during therapeutic gene transfer. Proc. Natl. Acad. Sci. USA *106*, 10770–10774.

28. Shi, D., Morizono, H., Ha, Y., Aoyagi, M., Tuchman, M., and Allewell, N.M. (1998). 1.85-A resolution crystal structure of human ornithine transcarbamoylase complexed with N-phosphonacetyl-L-ornithine. Catalytic mechanism and correlation with inherited deficiency. J. Biol. Chem. *273*, 34247–34254.

29. Shi, D., Morizono, H., Yu, X., Tong, L., Allewell, N.M., and Tuchman, M. (2001). Human ornithine transcarbamylase: crystallographic insights into substrate recognition and conformational changes. Biochem. J. *354*, 501–509.

30. DeMars, R., LeVan, S.L., Trend, B.L., and Russell, L.B. (1976). Abnormal ornithine carbamoyltransferase in mice having the sparse-fur mutation. Proc. Natl. Acad. Sci. USA *73*, 1693–1697.

31. Hodges, P.E., and Rosenberg, L.E. (1989). The spfash mouse: a missense mutation in the ornithine transcarbamylase gene also causes aberrant mRNA splicing. Proc. Natl. Acad. Sci. USA *86*, 4142–4146.

32. Crawley, J.N. (2007). What's Wrong With My Mouse?: Behavioral Phenotyping of Transgenic and Knockout Mice (Wiley).

33. Ye, X., Robinson, M.B., Pabin, C., Quinn, T., Jawad, A., Wilson, J.M., and Batshaw, M.L. (1997). Adenovirus-mediated in vivo gene transfer rapidly protects ornithine transcarbamylase-deficient mice from an ammonium challenge. Pediatr. Res. *41*, 527–534.

34. Campbell, A.G., Rosenberg, L.E., Snodgrass, P.J., and Nuzum, C.T. (1973). Ornithine transcarbamylase deficiency: a cause of lethal neonatal hyperammonemia in males. N. Engl. J. Med. *288*, 1–6.

35. McCarty, D.M., Young, S.M., Jr., and Samulski, R.J. (2004). Integration of adeno-associated virus (AAV) and recombinant AAV vectors. Annu. Rev. Genet. *38*, 819–845.

36. Russell, D.W., Miller, A.D., and Alexander, I.E. (1994). Adeno-associated virus vectors preferentially transduce cells in S phase. Proc. Natl. Acad. Sci. USA *91*, 8915–8919.

37. Chandler, R.J., Sands, M.S., and Venditti, C.P. (2017). Recombinant Adeno-Associated Viral Integration and Genotoxicity: Insights from Animal Models. Hum. Gene Ther. *28*, 314–322.

38. Verdera, H.C., Kuranda, K., and Mingozzi, F. (2020). AAV Vector Immunogenicity in Humans: A Long Journey to Successful Gene Transfer. Mol. Ther. *28*, 723–746.

39. Muro, A.F., D'Antiga, L., and Mingozzi, F. (2018). Gene therapy in pediatric liver disease. In Pediatric Hepatology and Liver Transplantation, L. D'Antiga, ed. (Springer), pp. 799–829.

40. Bortolussi, G., Zentillin, L., Vaníkova, J., Bockor, L., Bellarosa, C., Mancarella, A., Vianello, E., Tiribelli, C., Giacca, M., Vitek, L., and Muro, A.F. (2014). Life-long correction of hyperbilirubinemia with a neonatal liver-specific AAV-mediated gene transfer in a lethal mouse model of Crigler-Najjar Syndrome. Hum. Gene Ther. *25*, 844–855.

41. Cunningham, S.C., Dane, A.P., Spinoulas, A., Logan, G.J., and Alexander, I.E. (2008). Gene delivery to the juvenile mouse liver using AAV2/8 vectors. Mol. Ther. *16*, 1081–1088.

42. Wang, L., Wang, H., Bell, P., McMenamin, D., and Wilson, J.M. (2012). Hepatic gene transfer in neonatal mice by adeno-associated virus serotype 8 vector. Hum. Gene Ther. *23*, 533–539.

43. Mingozzi, F., and High, K.A. (2017). Overcoming the Host Immune Response to Adeno-Associated Virus Gene Delivery Vectors: The Race Between Clearance, Tolerance, Neutralization, and Escape. Annu. Rev. Virol. *4*, 511–534.

44. Ronzitti, G., Gross, D.A., and Mingozzi, F. (2020). Human Immune Responses to Adeno-Associated Virus (AAV) Vectors. Front. Immunol. *11*, 670.

45. Murphy, S.L., Li, H., Mingozzi, F., Sabatino, D.E., Hui, D.J., Edmonson, S.A., and High, K.A. (2009). Diverse IgG subclass responses to adeno-associated virus infection and vector administration. J. Med. Virol. *81*, 65–74.

46. Kishimoto, T.K., Ferrari, J.D., LaMothe, R.A., Kolte, P.N., Griset, A.P., O'Neil, C., Chan, V., Browning, E., Chalishazar, A., Kuhlman, W., et al. (2016). Improving the efficacy and safety of biologic drugs with tolerogenic nanoparticles. Nat. Nanotechnol. *11*, 890–899.

47. Maldonado, R.A., LaMothe, R.A., Ferrari, J.D., Zhang, A.H., Rossi, R.J., Kolte, P.N., Griset, A.P., O'Neil, C., Altreuter, D.H., Browning, E., et al. (2015). Polymeric synthetic nanoparticles for the induction of antigen-specific immunological tolerance. Proc. Natl. Acad. Sci. USA *112*, E156–E165.

48. Meliani, A., Boisgerault, F., Hardet, R., Marmier, S., Collaud, F., Ronzitti, G., Leborgne, C., Costa Verdera, H., Simon Sola, M., Charles, S., et al. (2018). Antigen-selective modulation of AAV immunogenicity with tolerogenic rapamycin nanoparticles enables successful vector re-administration. Nat. Commun. *9*, 4098.

49. Leborgne, C., Barbon, E., Alexander, J.M., Hanby, H., Delignat, S., Cohen, D.M., Collaud, F., Muraleetharan, S., Lupo, D., Silverberg, J., et al. (2020). IgG-cleaving endopeptidase enables in vivo gene therapy in the presence of anti-AAV neutralizing antibodies. Nat. Med. *26*, 1096–1101.

50. Bertin, B., Veron, P., Leborgne, C., Deschamps, J.Y., Moullec, S., Fromes, Y., Collaud, F., Boutin, S., Latournerie, V., van Wittenberghe, L., et al. (2020). Capsid-specific removal of circulating antibodies to adeno-associated virus vectors. Sci. Rep. *10*, 864.

51. Chicoine, L.G., Montgomery, C.L., Bremer, W.G., Shontz, K.M., Griffin, D.A., Heller, K.N., Lewis, S., Malik, V., Grose, W.E., Shilling, C.J., et al. (2014). Plasmapheresis eliminates the negative impact of AAV antibodies on microdystrophin gene expression following vascular delivery. Mol. Ther. *22*, 338–347.

52. Collaud, F., Bortolussi, G., Guianvarc'h, L., Aronson, S.J., Bordet, T., Veron, P., Charles, S., Vidal, P., Sola, M.S., Rundwasser, S., et al. (2018). Preclinical Development of an AAV8-hUGT1A1 Vector for the Treatment of Crigler-Najjar Syndrome. Mol. Ther. Methods Clin. Dev. *12*, 157–174.

53. Ayuso, E., Mingozzi, F., Montane, J., Leon, X., Anguela, X.M., Haurigot, V., Edmonson, S.A., Africa, L., Zhou, S., High, K.A., et al. (2010). High AAV vector purity results in serotype- and tissue-independent enhancement of transduction efficiency. Gene Ther. *17*, 503–510.

54. Matsushita, T., Elliger, S., Elliger, C., Podsakoff, G., Villarreal, L., Kurtzman, G.J., Iwaki, Y., and Colosi, P. (1998). Adeno-associated virus vectors can be efficiently produced without helper virus. Gene Ther. *5*, 938–945.

55. Ye, X., Robinson, M.B., Batshaw, M.L., Furth, E.E., Smith, I., and Wilson, J.M. (1996). Prolonged metabolic correction in adult ornithine transcarbamylase-deficient mice with adenoviral vectors. J. Biol. Chem. *271*, 3639–3646.

OMTM, Volume *20*

Supplemental Information

Long-term correction of ornithine transcarbamylase deficiency in Spf-Ash mice with a translationally optimized AAV vector

Giulia De Sabbata, Florence Boisgerault, Corrado Guarnaccia, Alessandra Iaconcig, Giulia Bortolussi, Fanny Collaud, Giuseppe Ronzitti, Marcelo Simon Sola, Patrice Vidal, Jeremy Rouillon, Severine Charles, Emanuele Nicastro, Lorenzo D'Antiga, Petr Ilyinskii, Federico Mingozzi, Takashi Kei Kishimoto, and Andrés F. Muro

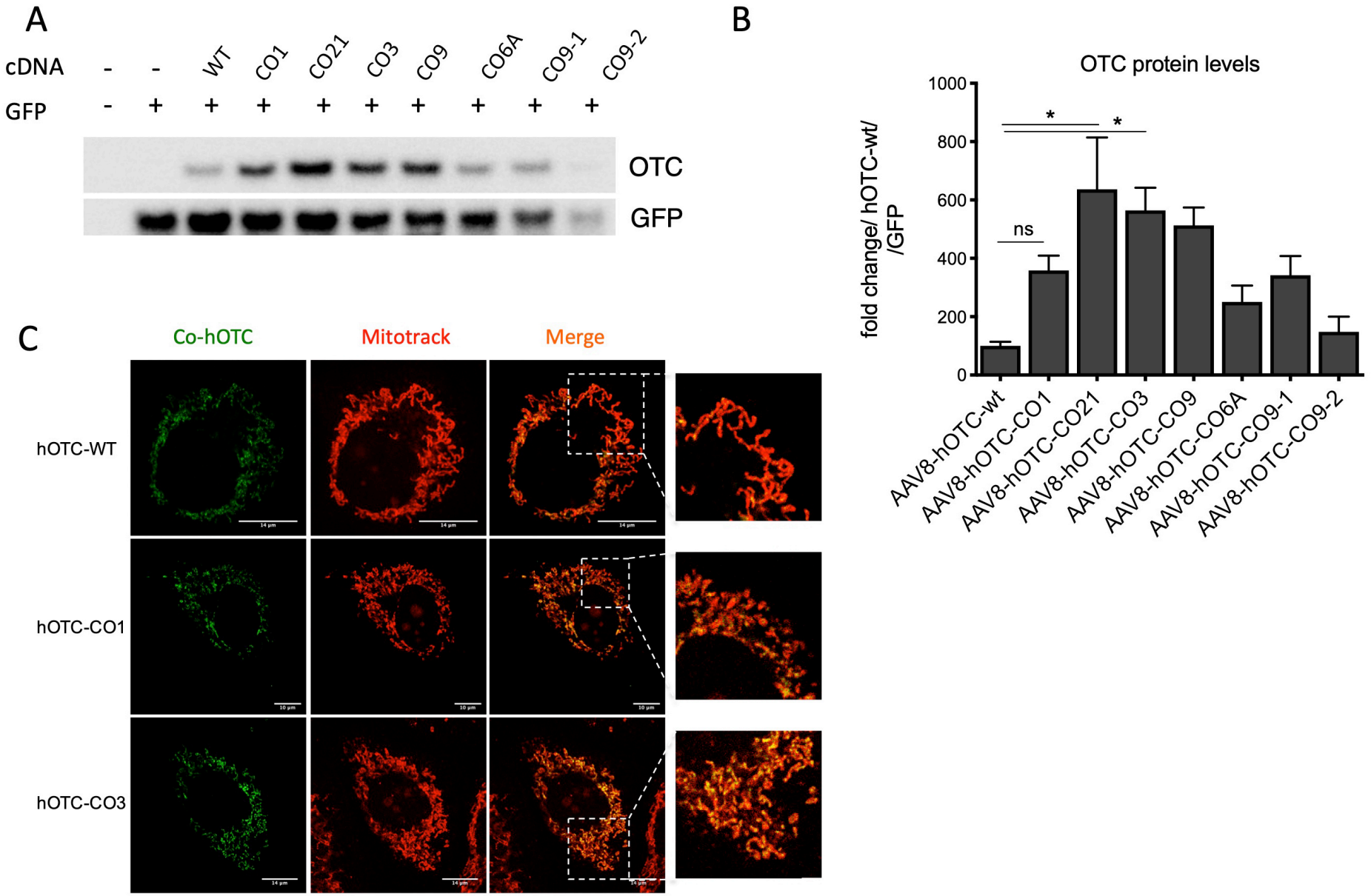

Figure S1. Codon-optimized hOTC variants tested in Huh-7 human liver cells. A) Representative Western blot analysis of OTC protein levels in cell lysates (15 µg protein per lane) following co-transfection of pSMD2-hOTC-CO constructs and GPF plasmid. The control lane contains cell lysate from non-transfected cells, while the empty lane contains lysate from cells transfected with empty AAV8 plasmid (pSMD2) together with GFP plasmid. **B)** Densitometric quantification of OTC protein from the experiment shown in Panel A. GFP was used as transfection control. Values are expressed as fold-change respect to the AAV8-hOTC-wt. Data are shown as mean ± SEM and statistical analyses was performed by one-way ANOVA with Turkey's Multiple comparison test (n=2, *P <0,05). **C)** Sub-cellular localization studies of hOTC in Huh-7 human liver cells. Huh-7 cells were transfected with plasmids encoding the indiacted hOTC-CO variants. Mitochondria (red, MITO-TRACK) and hOTC (green) were detected with a confocal microscope. On the right, a magnified picture of the indicated areas is shown. The scale bar corresponds to 14 µm.

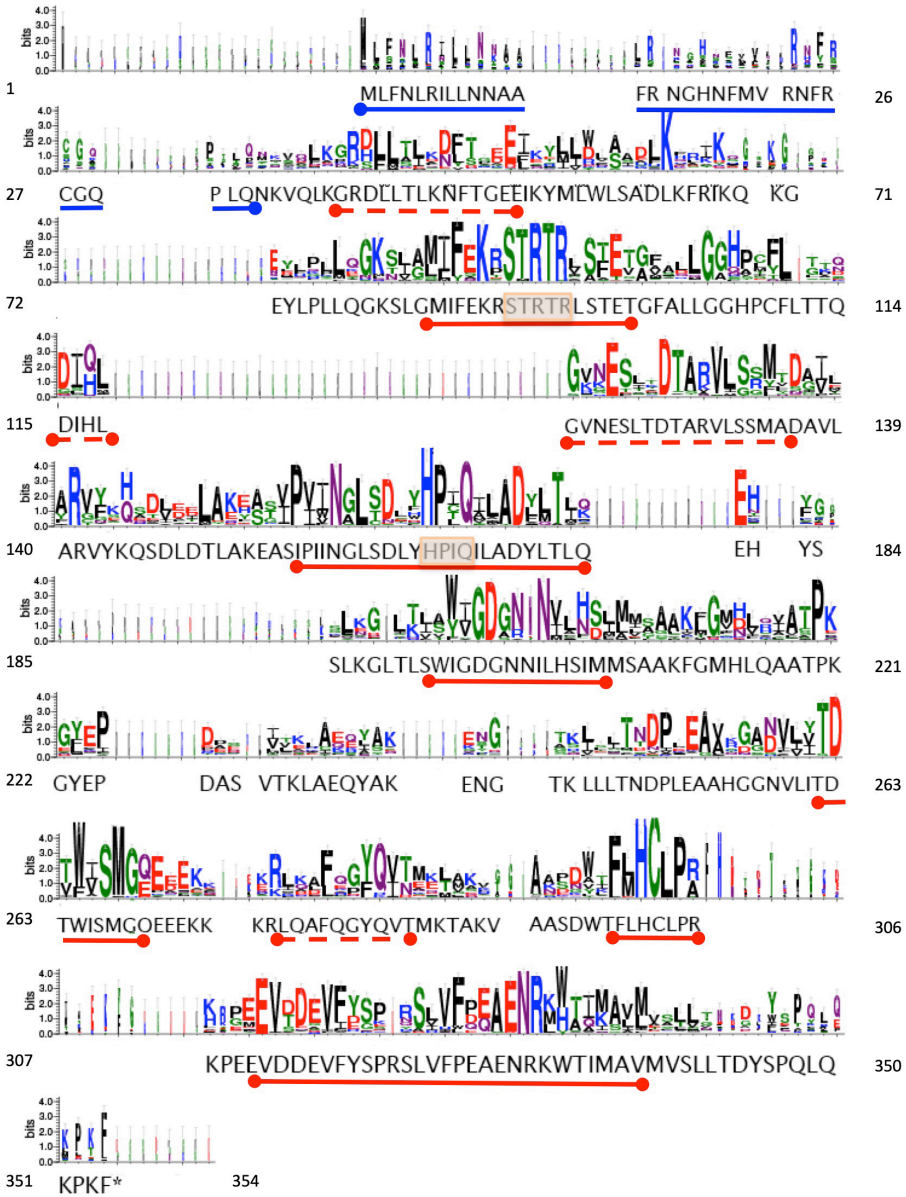

Figure S2. **Logo representation of the alignment of 142 OTCases.** The size of the letters indicates the degree of sequence conservation and most of these have catalytically or structurally important roles. The human full-length OTC primary sequence is shown below the logo. The signal peptide and mitochondrial localization sequence are indicated by a blue line below the human sequence. Very conserved regions are indicated by a red continuous line, while the dashed line indicate conserved regions. The active sites are indicated by an orange rectangle (90-94 and 160-171: Ornithine and carbamoyl phosphate binding site, respectively). The numbers at the side (from 1 to 354) correspond to the human OTC amino acidic sequence. Gaps in the human sequence are caused by insertions in the OTC cDNAs in the different species, resulting in different-length sequences. Table S1 contains the list of species used in the representation.

5′

ATGCTGTTCAACCTGCGAATCCTGCTGAACAACGCCGCTTTTCGGAACGGGCACAAC
TTTATGGTGAGGAACTTTCGCTGCGGACAGCCCCTCCAGAATAAGGTCCAGCTGAAG
GGCAGGGACCTGCTGACCCTGAAAAATTTCACAGGGGAGGAAATCAAATACATGCTG
TGGCTGAGCGCCGATCTGAAGTTCAGAATCAAGCAGAAGGGCGAGTACCTGCCTCTG
CTCCAGGGCAAAAGCCTGGGGATGATCTTCGAAAAGCGCAGTACTCGGACCAGACTG
TCAACCGAGACTGGCTTCGCTCTGCTGGGAGGCCACCCTTGCTTCCTGACAACCCAG
GACATTCACCTGGGAGTGAACGAGTCCCTGACCGACACTGCTCGCGTCCTGAGCTCT
ATGGCCGACGCCGTGCTGGCTCGGGTGTACAAACAGTCCGACCTGGATACCCTGGCC
AAGGAAGCTTCCATCCCCATCATCAACGGCCTGAGCGACCTGTACCACCCCATCCAG
ATCCTGGCCGACTACCTGACCCTGCAGGAGCACTACAGCAGCCTGAAGGGCCTGACC
CTGAGCTGGATCGGCGACGGCAACAATATCCTGCACTCTATTATGATGTCTGCCGCC
AAGTTTGGAATGCACCTGCAGGCTGCTACCCCTAAAGGCTACGAACCCGATGCCTCT
GTGACAAAGCTGGCTGAACAGTACGCCAAAGAGAACGGCACAAAGCTGCTGCTGACC
AACGACCCTCTGGAGGCCGCTCACGGAGGCAACGTGCTGATCACCGATACCTGGATT
AGTATGGGACAGGAGGAAGAGAAGAAGAAGCGGCTGCAGGCCTTCCAGGGCTACCAG
GTCACCATGAAAACCGCTAAGGTGGCCGCCAGCGATTGGACCTTTCTGCACTGCCTG
CCCAGAAAGCCCGAAGAGGTGGACGACGAGGTCTTCTACTCTCCCAGAAGCCTGGTG
TTTCCCGAAGCTGAGAATAGGAAGTGGACAATTATGGCAGTGATGGTGTCCCTGCTG
ACTGATTATTCTCCTCAACTGCAGAAACCTAAATTTTGA

3′

Figure S3. **Nucleotide sequence of the codon optimized hOTC CO21 ORF.** The 5′ and 3′ orientation of the sequence are indicated.

A

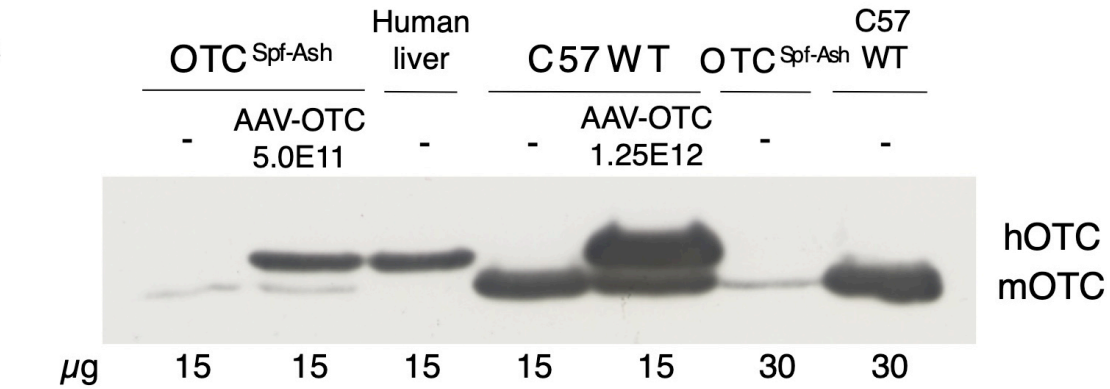

B

```
Alignment of Sequence_1:  [OTC-001 cds.xprt] with  Sequence_2: [mOTC ORF.xprt]

Similarity : 345/353 (97.73 %)

Seq_1  1     MLFNLRILLNNAAFRNGHNFMVRNFRCGQPLQNKVQLKGRDLLTLKNFTGEEIKYMLWLS  60
             ||:||||||||||:|:||:::||:|:||:|:|: |||||||||||||||||||| ||||||
Seq_2  1     MLSNLRILLNNAALRKGHTSVVRHFWCGKPVQSQVQLKGRDLLTLKNFTGEEIQYMLWLS  60

Seq_1  61    ADLKFRIKQKGEYLPLLQGKSLGMIFEKRSTRTRLSTETGFALLGGHPCFLTTQDIHLGV  120
             ||||||||||||||||||||||||||||||||||||||||||||||||||| ||||||||||
Seq_2  61    ADLKFRIKQKGEYLPLLQGKSLGMIFEKRSTRTRLSTETGFALLGGHPSFLTTQDIHLGV  120

Seq_1  121   NESLTDTARVLSSMADAVLARVYKQSDLDTLAKEASIPIINGLSDLYHPIQILADYLTLQ  180
             |||||||||||||| |||||||||||||||||||||| ||||||||||||||||||||||
Seq_2  121   NESLTDTARVLSSMTDAVLARVYKQSDLDTLAKEASIPIVNGLSDLYHPIQILADYLTLQ  180

Seq_1  181   EHYSSLKGLTLSWIGDGNNILHSIMMSAAKFGMHLQAATPKGYEPD-ASVTKLAEQYAKE  239
             ||| |||||||||||||||||||||||||||||||||||||||||| : | |||||||||
Seq_2  181   EHYGSLKGLTLSWIGDGNNILHSIMMSAAKFGMHLQAATPKGYEPDPNIV-KLAEQYAKE  239

Seq_1  240   NGTKLLLTNDPLEAAHGGNVLITDTWISMGQEEEKKKRLQAFQGYQVTMKTAKVAASDWT  299
             |||||::|||||||||:|||||||||||||||| ||||||||||||||||||||||||||
Seq_2  240   NGTKLSMTNDPLEAARGGNVLITDTWISMGQEDEKKKRLQAFQGYQVTMKTAKVAASDWT  299

Seq_1  300   FLHCLPRKPEEVDDEVFYSPRSLVFPEAENRKWTIMAVMVSLLTDYSPQLQKPKF  354
             |||||||||||||||||||||||||||||||||||||||||||||||||||:||||||
Seq_2  300   FLHCLPRKPEEVDDEVFYSPRSLVFPEAENRKWTIMAVMVSLLTDYSPVLQKPKF  354
```

Figure S4. Comparison of human and mouse OTC proteins. A) The same amounts of liver protein extracts from mice (OTC^{SpfAsh} and WT C57Bl/6) non-transduced or transduced (with rAAV8-OTC-CO3), and human liver protein extract were run in an SDS-PAGE and the OTC protein detected by WB. Fifteen (15 µg) or thirty micrograms (30 µg) of protein extract were loaded. Adult OTC^{SpfAsh} and WT C57Bl/6 male mice were i.v. transduced with 5.0E11 vg/kg and 1.25E12 vg/kg, respectively; **B)** Alignment of the human (Seq_1) and mouse (Seq_2) OTC primary sequences.

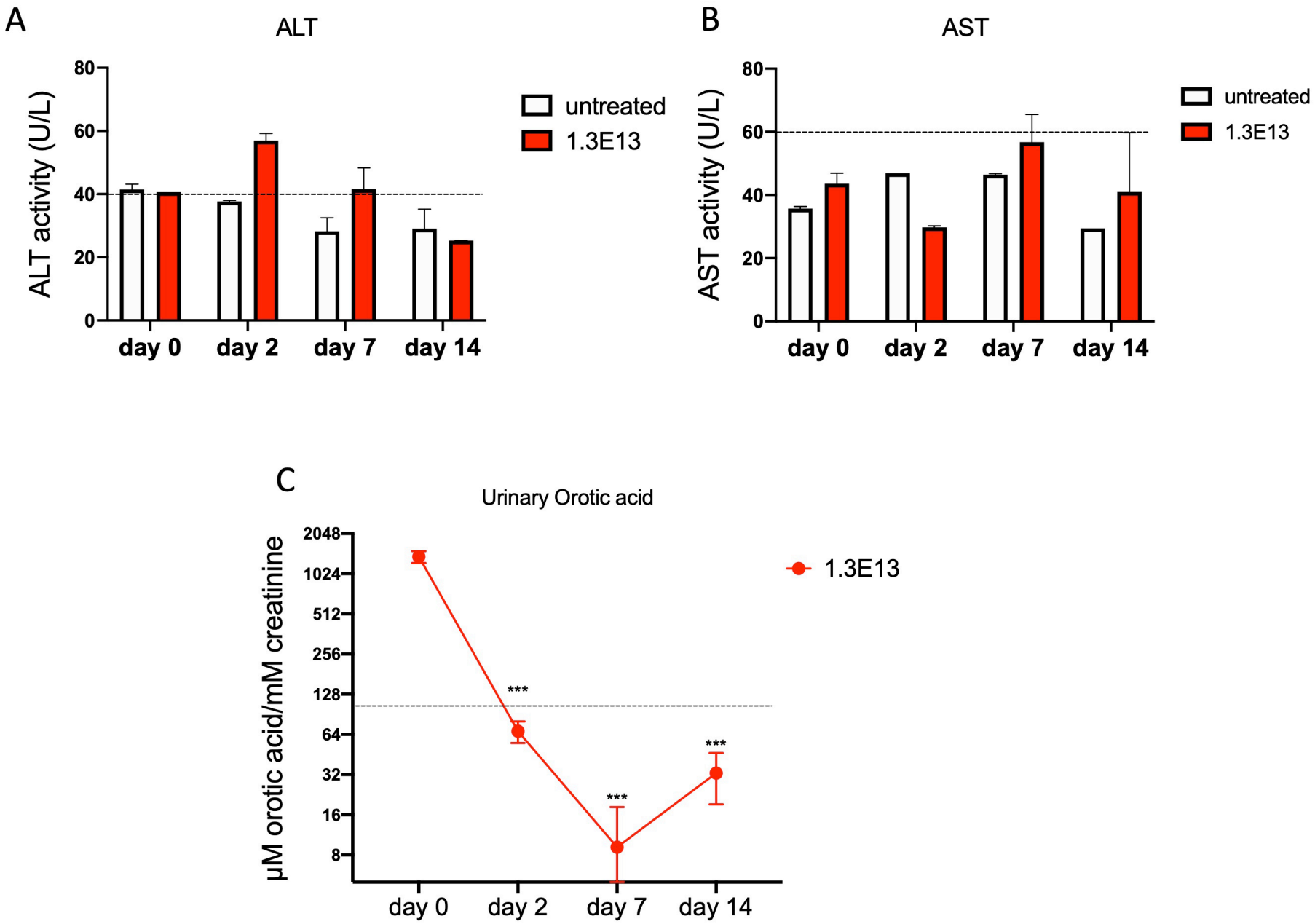

Figure S5. High dose treatment. Analysis of liver transaminases in plasma. Juvenile P30 OTC^{SpfAsh} mice were i.v. injected with 1.3E13 vg/kg of the or AAV8-hOTC-CO21Δice were i.v. inj2). Blood samples were taken at 2, 7 and 14 days after vector administration. AST **(A)**, ALT **(B)** liver transaminases, and urinary orotic acid **(C)** were determined. Data are shown as mean ± SEM and statistical analyses was performed by two-way ANOVA with mixed effect analysis for Panels A and B, and with one-way ANOVA with Bonferroni's multiple comparison test (***P <0,0001).

Table S1. List of 142 species from which the ornithine transcarbalylase (ornithine carbamoyltransferase, OTCase) primary sequence were obtained. These sequences were then aligned to generate the logo representation of Figure S2.

Entry	Entry name	Status	Protein names	Gene names	Organism	Length
P18186	OTC_BACSU	reviewed	Ornithine carbamoyltransferase (OTCase) (EC 2.1.3.3)	argF BSU11250	Bacillus subtilis (strain 168)	319
O19072	OTC_PIG	reviewed	Ornithine carbamoyltransferase, mitochondrial (EC 2.1.3.3) (Ornithine	OTC	Sus scrofa (Pig)	328
Q0SM07	OTC_BORAP	reviewed	Ornithine carbamoyltransferase (OTCase) (EC 2.1.3.3)	arcB BAPKO_0897 BafPKo_0870	Borrelia afzelii (strain PKo)	328
E6N013	OTC_NEIMH	reviewed	Ornithine carbamoyltransferase (OTCase) (EC 2.1.3.3)	argF NMBH4476_0658 NMH_2186	Neisseria meningitidis serogroup B / serotype 15 (strain H44/76)	331
P11803	OTC_EMENI	reviewed	Ornithine carbamoyltransferase, mitochondrial (EC 2.1.3.3) (Ornithine	argB AN4409	Emericella nidulans (strain FGSC A4 / ATCC 38163 / CBS 112.46 / NRRL 194 / M139) (Aspergillus nidulan	359
P65601	OTCC_STAAM	reviewed	Ornithine carbamoyltransferase, catabolic (OTCase) (EC 2.1.3.3)	arcB SAV2634	Staphylococcus aureus (strain Mu50 / ATCC 700699)	336
P31317	OTC_SCHPO	reviewed	Ornithine carbamoyltransferase, mitochondrial (EC 2.1.3.3) (Ornithine	arg3 SPAC4G9.10	Schizosaccharomyces pombe (strain 972 / ATCC 24843) (Fission yeast)	327
P11066	OTC_ASPNG	reviewed	Ornithine carbamoyltransferase, mitochondrial (EC 2.1.3.3) (Ornithine	argB	Aspergillus niger	370
B1KXQ3	OTC_CLOBM	reviewed	Ornithine carbamoyltransferase (OTCase) (EC 2.1.3.3)	arcB CLK_1978	Clostridium botulinum (strain Loch Maree / Type A3)	333
P11725	OTC_MOUSE	reviewed	Ornithine carbamoyltransferase, mitochondrial (EC 2.1.3.3) (Ornithine	Otc	Mus musculus (Mouse)	354
P0CL21	OTC_COCIM	reviewed	Ornithine carbamoyltransferase, mitochondrial (EC 2.1.3.3) (Ornithine	CIMG_04084	Coccidioides immitis (strain RS) (Valley fever fungus)	349
P31326	OTC_LITCT	reviewed	Ornithine carbamoyltransferase, mitochondrial (EC 2.1.3.3) (Ornithine transcarbamylase) (OTCase)		Lithobates catesbeianus (American bullfrog) (Rana catesbeiana)	350
Q8CMW2	OTCC2_STAES	reviewed	Ornithine carbamoyltransferase 2, catabolic (OTCase 2) (EC 2.1.3.3)	arcB2 SE_2216	Staphylococcus epidermidis (strain ATCC 12228)	335
Q9YHY9	OTC_CHICK	reviewed	Ornithine carbamoyltransferase, mitochondrial (EC 2.1.3.3) (Ornithine	OTC	Gallus gallus (Chicken)	354
O50039	OTC_ARATH	reviewed	Ornithine carbamoyltransferase, chloroplastic (EC 2.1.3.3) (Ornithine t	OTC At1g75330 F1B16.13	Arabidopsis thaliana (Mouse-ear cress)	375
A6QG68	OTC_STAAE	reviewed	Ornithine carbamoyltransferase (OTCase) (EC 2.1.3.3)	argF NWMN_1078	Staphylococcus aureus (strain Newman)	333
Q1JFZ1	OTC_STRPD	reviewed	Ornithine carbamoyltransferase (OTCase) (EC 2.1.3.3)	arcB MGAS10270_Spy1288	Streptococcus pyogenes serotype M2 (strain MGAS10270)	337
Q8G998	OTCC_LACHI	reviewed	Ornithine carbamoyltransferase, catabolic (OTCase) (EC 2.1.3.3)	arcB	Lactobacillus hilgardii	343
P04391	OTC1_ECOLI	reviewed	Ornithine carbamoyltransferase subunit I (OTCase-1) (EC 2.1.3.3)	argI b4254 JW4211	Escherichia coli (strain K12)	334
Q3J4X5	OTC_RHOS4	reviewed	Ornithine carbamoyltransferase (OTCase) (EC 2.1.3.3)	argF RHOS4_05910 RSP_2009	Rhodobacter sphaeroides (strain ATCC 17023 / 2.4.1 / NCIB 8253 / DSM 158)	308
Q8ET05	OTC_OCEIH	reviewed	Ornithine carbamoyltransferase (OTCase) (EC 2.1.3.3)	argF OB0460	Oceanobacillus iheyensis (strain DSM 14371 / CIP 107618 / JCM 11309 / KCTC 3954 / HTE831)	322
Q8CU41	OTCC1_STAES	reviewed	Ornithine carbamoyltransferase 1, catabolic (OTCase 1) (EC 2.1.3.3)	arcB1 SE_0103	Staphylococcus epidermidis (strain ATCC 12228)	332
P14995	OTC_PACTA	reviewed	Ornithine carbamoyltransferase, mitochondrial (EC 2.1.3.3) (Ornithine	OTC	Pachysolen tannophilus (Yeast)	347
P65603	OTCC1_STRA3	reviewed	Ornithine carbamoyltransferase 1, catabolic (OTCase 1) (EC 2.1.3.3)	arcB1 gbs2085	Streptococcus agalactiae serotype III (strain NEM316)	332
P00481	OTC_RAT	reviewed	Ornithine carbamoyltransferase, mitochondrial (EC 2.1.3.3) (Ornithine	Otc	Rattus norvegicus (Rat)	354
P65605	OTCC2_STRA3	reviewed	Ornithine carbamoyltransferase 2, catabolic (OTCase 2) (EC 2.1.3.3)	arcB2 gbs2124	Streptococcus agalactiae serotype III (strain NEM316)	337
P84010	OTC_SHEEP	reviewed	Ornithine carbamoyltransferase, mitochondrial (EC 2.1.3.3) (Ornithine	OTC	Ovis aries (Sheep)	355
B5XMC1	OTC_STRPZ	reviewed	Ornithine carbamoyltransferase (OTCase) (EC 2.1.3.3)	arcB Spy49_1195c	Streptococcus pyogenes serotype M49 (strain NZ131)	337
Q48296	OTCC_HALSA	reviewed	Ornithine carbamoyltransferase, catabolic (cOTCase) (EC 2.1.3.3)	arcB argB VNG_6315G	Halobacterium salinarum (strain ATCC 700922 / JCM 11081 / NRC-1) (Halobacterium halobium)	295
P0C2P2	OTC_ASPTE	reviewed	Ornithine carbamoyltransferase, mitochondrial (EC 2.1.3.3) (Ornithine	arg1 arg-1	Aspergillus terreus	361
Q9PNU6	OTCA_CAMJE	reviewed	Ornithine carbamoyltransferase, anabolic (OTCase) (EC 2.1.3.3)	argF CJ0994c	Campylobacter jejuni subsp. jejuni serotype O:2 (strain ATCC 700819 / NCTC 11168)	306
Q43814	OTC_PEA	reviewed	Ornithine carbamoyltransferase, chloroplastic (EC 2.1.3.3) (Ornithine t	ARGF	Pisum sativum (Garden pea)	375
Q02047	OTC1A_PSESH	reviewed	Ornithine carbamoyltransferase 1, anabolic (OTCase 1) (EC 2.1.3.3) (O	argF	Pseudomonas savastanoi pv. phaseolicola (Pseudomonas syringae pv. phaseolicola)	306
A4VU03	OTC_STRSY	reviewed	Ornithine carbamoyltransferase (OTCase) (EC 2.1.3.3)	arcB SSU05_0626	Streptococcus suis (strain 05ZYH33)	337
P00480	OTC_HUMAN	reviewed	Ornithine carbamoyltransferase, mitochondrial (EC 2.1.3.3) (Ornithine	OTC	Homo sapiens (Human)	354
P65604	OTCC1_STRA5	reviewed	Ornithine carbamoyltransferase 1, catabolic (OTCase 1) (EC 2.1.3.3)	arcB1 SAG2126	Streptococcus agalactiae serotype V (strain ATCC BAA-611 / 2603 V/R)	332
Q9N1U7	OTC_BOVIN	reviewed	Ornithine carbamoyltransferase, mitochondrial (EC 2.1.3.3) (Ornithine	OTC	Bos taurus (Bovine)	354
Q2YPH2	OTC_BRUA2	reviewed	Ornithine carbamoyltransferase (OTCase) (EC 2.1.3.3)	arcB BAB1_0332	Brucella abortus (strain 2308)	312
Q97ZM1	OTC_SACS2	reviewed	Ornithine carbamoyltransferase (OTCase) (EC 2.1.3.3)	argF SSO0871	Saccharolobus solfataricus (strain ATCC 35092 / DSM 1617 / JCM 11322 / P2) (Sulfolobus solfataricus)	307
P44770	OTCC_HAEIN	reviewed	Ornithine carbamoyltransferase, catabolic (OTCase) (EC 2.1.3.3)	arcB HI_0596	Haemophilus influenzae (strain ATCC 51907 / DSM 11121 / KW20 / Rd)	334
P68746	OTC2_PSESF	reviewed	Ornithine carbamoyltransferase 2, phaseolotoxin-insensitive (OTCase	argK	Pseudomonas syringae pv. actinidiae	327
P78605	OTC_TRAHI	reviewed	Ornithine carbamoyltransferase, mitochondrial (EC 2.1.3.3) (Ornithine	transcarbamylase) (OTCase)	Trametes hirsuta (White-rot fungus) (Coriolus hirsutus)	375
P68747	OTC2A_PSESH	reviewed	Ornithine carbamoyltransferase 2, anabolic (OTCase 2) (EC 2.1.3.3) (O	argK	Pseudomonas savastanoi pv. phaseolicola (Pseudomonas syringae pv. phaseolicola)	327
Q1JAR4	OTC_STRPB	reviewed	Ornithine carbamoyltransferase (OTCase) (EC 2.1.3.3)	arcB MGAS2096_Spy1292	Streptococcus pyogenes serotype M12 (strain MGAS2096)	337
P06960	OTC2_ECOLI	reviewed	Ornithine carbamoyltransferase subunit F (OTCase-2) (EC 2.1.3.3)	argF b0273 JW0266	Escherichia coli (strain K12)	334
P65606	OTCC2_STRA5	reviewed	Ornithine carbamoyltransferase 2, catabolic (OTCase 2) (EC 2.1.3.3)	arcB2 SAG2165	Streptococcus agalactiae serotype V (strain ATCC BAA-611 / 2603 V/R)	337
P0C2P3	OTC_ASPTN	reviewed	Ornithine carbamoyltransferase, mitochondrial (EC 2.1.3.3) (Ornithine	arg1 arg-1 ATEG_05492	Aspergillus terreus (strain NIH 2624 / FGSC A1156)	361
P11724	OTCA_PSEAE	reviewed	Ornithine carbamoyltransferase, anabolic (OTCase) (EC 2.1.3.3)	argF PA3537	Pseudomonas aeruginosa (strain ATCC 15692 / DSM 22644 / CIP 104116 / JCM 14847 / LMG 12228 / 1C	305
Q51742	OTCA_PYRFU	reviewed	Ornithine carbamoyltransferase, anabolic (OTCase) (EC 2.1.3.3)	argF PF0594	Pyrococcus furiosus (strain ATCC 43587 / DSM 3638 / JCM 8422 / Vc1)	315
A0A2L2X5J4	A0A2L2X5J4_9BACT	unreviewed	Ornithine carbamoyltransferase (OTCase) (EC 2.1.3.3)	OTC tpqmel_0752	Candidatus Gastranaerophilus sp. (ex Termes propinquus)	310
D8LLH5	D8LLH5_ECTSI	unreviewed	Ornithine transcarbamoylase (EC 2.1.3.3)	OTC Esi_0361_0020	Ectocarpus siliculosus (Brown alga) (Conferva siliculosa)	320
A0A367YH05	A0A367YH05_9ASCO	unreviewed	Ornithine carbamoyltransferase, mitochondrial	OTC Cantr_00823	Candida viswanathii	343
A0A4X1U355	A0A4X1U355_PIG	unreviewed	Ornithine carbamoyltransferase, mitochondrial	OTC	Sus scrofa (Pig)	354
A0A2U4C0Z2	A0A2U4C0Z2_TURTR	unreviewed	ornithine carbamoyltransferase, mitochondrial	OTC	Tursiops truncatus (Atlantic bottle-nosed dolphin) (Delphinus truncatus)	354
A0A340WRA1	A0A340WRA1_LIPVE	unreviewed	ornithine carbamoyltransferase, mitochondrial	OTC	Lipotes vexillifer (Yangtze river dolphin)	354
A0A2Y9FRK9	A0A2Y9FRK9_PHYMC	unreviewed	ornithine carbamoyltransferase, mitochondrial	OTC	Physeter macrocephalus (Sperm whale) (Physeter catodon)	354
A0A2Y9GIU7	A0A2Y9GIU7_NEOSC	unreviewed	ornithine carbamoyltransferase, mitochondrial	OTC	Neomonachus schauinslandi (Hawaiian monk seal) (Monachus schauinslandi)	354
A0A142BFN0	A0A142BFN0_9GAMM	unreviewed	Ornithine carbamoyltransferase (OTCase) (EC 2.1.3.3)	otc EZMO1_3576	Endozoicomonas montiporae CL-33	338
A0A2B4SXF3	A0A2B4SXF3_STYPI	unreviewed	Ornithine carbamoyltransferase, mitochondrial	OTC AWC38_SpisGene422	Stylophora pistillata (Smooth cauliflower coral)	376
A0A1U7R918	A0A1U7R918_ALLSI	unreviewed	ornithine carbamoyltransferase, mitochondrial	OTC	Alligator sinensis (Chinese alligator)	354
Q9IAU8	Q9IAU8_TRASE	unreviewed	Ornithine transcarbamylase	OTC	Trachemys scripta elegans (Red-eared slider turtle)	354
W5UIC6	W5UIC6_ICTPU	unreviewed	Ornithine carbamoyltransferase, mitochondrial	OTC	Ictalurus punctatus (Channel catfish) (Silurus punctatus)	352
A0A1Y2FGM4	A0A1Y2FGM4_PROLT	unreviewed	Ornithine carbamoyltransferase OTC/ARG3	BCR37DRAFT_379026	Protomyces lactucaedebilis	353
A0A2I2FBI7	A0A2I2FBI7_9EURO	unreviewed	Ornithine carbamoyltransferase OTC/ARG3	BDW47DRAFT_125699	Aspergillus candidus	365
M9ME20	M9ME20_PSEA3	unreviewed	Ornithine carbamoyltransferase OTC/ARG3	PANT_8c00049	Pseudozyma antarctica (strain T-34) (Yeast) (Candida antarctica)	382
A0A2U3YSD6	A0A2U3YSD6_LEPWE	unreviewed	ornithine carbamoyltransferase, mitochondrial	OTC	Leptonychotes weddellii (Weddell seal) (Otaria weddellii)	354
A0A3Q7SVY1	A0A3Q7SVY1_VULVU	unreviewed	ornithine carbamoyltransferase, mitochondrial	OTC	Vulpes vulpes (Red fox)	354
H2PVB0	H2PVB0_PONAB	unreviewed	Ornithine carbamoyltransferase	OTC	Pongo abelii (Sumatran orangutan) (Pongo pygmaeus abelii)	354
F1MNG5	F1MNG5_BOVIN	unreviewed	Ornithine carbamoyltransferase, mitochondrial	OTC	Bos taurus (Bovine)	354
H2QYG7	H2QYG7_PANTR	unreviewed	Ornithine carbamoyltransferase	OTC	Pan troglodytes (Chimpanzee)	354
A0A1S2ZR68	A0A1S2ZR68_ERIEU	unreviewed	ornithine carbamoyltransferase, mitochondrial	OTC	Erinaceus europaeus (Western European hedgehog)	354
A0A2Y9MVT8	A0A2Y9MVT8_DELLE	unreviewed	ornithine carbamoyltransferase, mitochondrial	OTC	Delphinapterus leucas (Beluga whale)	354
A0A480E1W6	A0A480E1W6_PIG	unreviewed	Ornithine carbamoyltransferase, mitochondrial	OTC	Sus scrofa (Pig)	354
I8TWB5	I8TWB5_ASPO3	unreviewed	Ornithine carbamoyltransferase OTC/ARG3	Ao3042_05393	Aspergillus oryzae (strain 3.042) (Yellow koji mold)	372
A0A1C7M8Y7	A0A1C7M8Y7_GRIFR	unreviewed	Ornithine carbamoyltransferase, mitochondrial	OTC A0H81_07006	Grifola frondosa (Maitake) (Polyporus frondosus)	342
G3AUC8	G3AUC8_SPAPN	unreviewed	Ornithine carbamoyltransferase OTC/ARG3	OTC/ARG3 SPAPADRAFT_63324	Spathaspora passalidarum (strain NRRL Y-27907 / 11-Y1)	331
A0A2HZZNI9	A0A2HZZNI9_9HYPO	unreviewed	Ornithine carbamoyltransferase OTC/ARG3	A9Z42_0081100	Trichoderma parareesei	353
A0A1D2VEQ1	A0A1D2VEQ1_9ASCO	unreviewed	Ornithine carbamoyltransferase OTC/ARG3	ASCRUDRAFT_36965	Ascoidea rubescens DSM 1968	335
A0A1T3CN33	A0A1T3CN33_9HYPO	unreviewed	Ornithine carbamoyltransferase OTC/ARG3	A0028_0036000	Trichoderma guizhouense	352
A0A2R8Y829	A0A2R8Y829_HUMAN	unreviewed	Ornithine carbamoyltransferase, mitochondrial	OTC	Homo sapiens (Human)	130
A0A3L6FRW5	A0A3L6FRW5_MAIZE	unreviewed	Ornithine carbamoyltransferase, chloroplastic	OTC Zm00014a_035572	Zea mays (Maize)	72
A0A2G9I100	A0A2G9I100_9LAMI	unreviewed	Ornithine carbamoyltransferase OTC/ARG3 (EC 2.1.3.3)	CDL12_03817	Handroanthus impetiginosus	261
A0A1J6ITD8	A0A1J6ITD8_NICAT	unreviewed	Ornithine carbamoyltransferase, chloroplastic	OTC A4A49_12784	Nicotiana attenuata (Coyote tobacco)	376
F8HE50	F8HE50_STRES	unreviewed	Ornithine carbamoyltransferase, catabolic (OTCase) (EC 2.1.3.3)	otc arcB Ssal_01556	Streptococcus salivarius (strain 57.I)	326
F1NUG7	F1NUG7_CHICK	unreviewed	Ornithine carbamoyltransferase, mitochondrial	OTC	Gallus gallus (Chicken)	354
Q9IAV1	Q9IAV1_9CHON	unreviewed	Ornithine transcarbamylase	OTC	Raja sp.	353
A0A178W4A4	A0A178W4A4_ARATH	unreviewed	OTC	AXX17_At1g69770	Arabidopsis thaliana (Mouse-ear cress)	375
F1RXQ9	F1RXQ9_PIG	unreviewed	Ornithine carbamoyltransferase, mitochondrial	OTC	Sus scrofa (Pig)	336
A0A3Q7N1Q8	A0A3Q7N1Q8_CALUR	unreviewed	ornithine carbamoyltransferase, mitochondrial	OTC	Callorhinus ursinus (Northern fur seal)	354
A0A341D0X9	A0A341D0X9_NEOAA	unreviewed	ornithine carbamoyltransferase, mitochondrial	OTC	Neophocaena asiaeorientalis asiaeorientalis (Yangtze finless porpoise) (Neophocaena phocaenoides sut	143
A0A2U3VWB6	A0A2U3VWB6_ODORO	unreviewed	ornithine carbamoyltransferase, mitochondrial	OTC	Odobenus rosmarus divergens (Pacific walrus)	354
A0A3Q7XZH7	A0A3Q7XZH7_URSAR	unreviewed	ornithine carbamoyltransferase, mitochondrial	OTC	Ursus arctos horribilis	354
A0A3833Z9Y7	A0A3833Z9Y7_BALAS	unreviewed	ornithine carbamoyltransferase, mitochondrial isoform X2	OTC	Balaenoptera acutorostrata scammoni (North Pacific minke whale) (Balaenoptera davidsoni)	299
A0A3833Z952	A0A3833Z952_BALAS	unreviewed	ornithine carbamoyltransferase, mitochondrial isoform X1	OTC	Balaenoptera acutorostrata scammoni (North Pacific minke whale) (Balaenoptera davidsoni)	354
A0A384CJU1	A0A384CJU1_URSMA	unreviewed	ornithine carbamoyltransferase, mitochondrial	OTC	Ursus maritimus (Polar bear) (Thalarctos maritimus)	354
V8NCN3	V8NCN3_OPHHA	unreviewed	Ornithine carbamoyltransferase, mitochondrial (Fragment)	OTC L345_14262	Ophiophagus hannah (King cobra) (Naja hannah)	292
Q9IAV0	Q9IAV0_SCEUN	unreviewed	Ornithine transcarbamylase	OTC	Sceloporus undulatus (Eastern fence lizard) (Stellio undulatus)	356
A0A1V4JC89	A0A1V4JC89_PATFA	unreviewed	Ornithine carbamoyltransferase, mitochondrial	OTC AV530_012700	Patagioenas fasciata monilis	335
Q9IAU7	Q9IAU7_PYTRG	unreviewed	Ornithine transcarbamylase (Fragment)	otc	Python regius (Ball python) (Boa regia)	163
Q5KTJ1	Q5KTJ1_CHICK	unreviewed	Ornithine transcarbamylase (Fragment)	OTC	Gallus gallus (Chicken)	18
Q59559	Q59559_MYCSP	unreviewed	Ornithine transcarbamylase (EC 2.1.3.3) (Fragment)	otc	Mycoplasma sp.	226
Q8R1A8	Q8R1A8_MOUSE	unreviewed	Ornithine carbamoyltransferase, mitochondrial (Otc protein)	Otc	Mus musculus (Mouse)	351
A0A3Q0D8F7	A0A3Q0D8F7_MESAU	unreviewed	ornithine carbamoyltransferase, mitochondrial	Otc	Mesocricetus auratus (Golden hamster)	354
A0A3L7H3E8	A0A3L7H3E8_CRIGR	unreviewed	OTC	CgPICR_014091	Cricetulus griseus (Chinese hamster) (Cricetulus barabensis griseus)	235
Q5M897	Q5M897_RAT	unreviewed	Otc protein	Otc	Rattus norvegicus (Rat)	350
A0A153G0L8	A0A153G0L8_DIPOR	unreviewed	ornithine carbamoyltransferase, mitochondrial	Otc	Dipodomys ordii (Ord's kangaroo rat)	355
G5BMQ9	G5BMQ9_HETGA	unreviewed	Ornithine carbamoyltransferase, mitochondrial	OTC GW7_05823	Heterocephalus glaber (Naked mole rat)	354
A1DS28	A1DS28_LACBU	unreviewed	Ornithine transcarbamylase (Fragment)	OTC	Lactobacillus buchneri	59
B8PV30	B8PV30_LACBR	unreviewed	Ornithine transcarbamylase (Fragment)	otc	Lactobacillus brevis	267
A1DS25	A1DS25_LACBR	unreviewed	Ornithine transcarbamylase (Fragment)	OTC	Lactobacillus brevis	60
A1DS22	A1DS22_PEDPE	unreviewed	Ornithine transcarbamylase (Fragment)	OTC	Pediococcus pentosaceus	55
A0A075HZ36	A0A075HZ36_9EURY	unreviewed	Ornithine carbamoyltransferase (OTC, argF, argI) (EC 2.1.3.3)	OTC argF argI	uncultured marine group II/III euryarchaeote KM3_87_G11	317
A0A075HNQ1	A0A075HNQ1_9EURY	unreviewed	Ornithine carbamoyltransferase (OTC, argF, argI) (EC 2.1.3.3)	OTC argF argI	uncultured marine group II/III euryarchaeote KM3_80_G12	220
A0A075FZ80	A0A075FZ80_9EURY	unreviewed	Ornithine carbamoyltransferase (OTC, argF, argI) (EC 2.1.3.3)	OTC argF argI	uncultured marine group II/III euryarchaeote AD1000_54_C05	319
A0A075FSL3	A0A075FSL3_9EURY	unreviewed	Ornithine carbamoyltransferase (OTC, argF, argI) (EC 2.1.3.3)	OTC argF argI	uncultured marine group II/III euryarchaeote AD1000_22_E05	316
A0A075HNS4	A0A075HNS4_9EURY	unreviewed	Ornithine carbamoyltransferase (OTC, argF, argI) (EC 2.1.3.3)	OTC argF argI	uncultured marine group II/III euryarchaeote KM3_72_E02	316
A0A075GRX7	A0A075GRX7_9EURY	unreviewed	Ornithine carbamoyltransferase (OTC, argF, argI) (EC 2.1.3.3)	OTC argF argI	uncultured marine group II/III euryarchaeote KM3_174_G08	316
A0A075FS77	A0A075FS77_9EURY	unreviewed	Ornithine carbamoyltransferase (OTC, argF, argI) (EC 2.1.3.3)	OTC argF argI	uncultured marine group II/III euryarchaeote AD1000_44_A09	316
A0A075HEL0	A0A075HEL0_9EURY	unreviewed	Ornithine carbamoyltransferase (OTC, argF, argI) (EC 2.1.3.3)	OTC argF argI	uncultured marine group II/III euryarchaeote KM3_63_C06	319
A0A075HAS3	A0A075HAS3_9EURY	unreviewed	Ornithine carbamoyltransferase (OTC, argF, argI) (EC 2.1.3.3)	OTC argF argI	uncultured marine group II/III euryarchaeote KM3_63_C07	319
A0A075H0L1	A0A075H0L1_9EURY	unreviewed	Ornithine carbamoyltransferase (OTC, argF, argI) (EC 2.1.3.3)	OTC argF argI	uncultured marine group II/III euryarchaeote KM3_31_G10	317
A0A075FKU7	A0A075FKU7_9EURY	unreviewed	Ornithine carbamoyltransferase (OTC, argF, argI) (EC 2.1.3.3)	OTC argF argI	uncultured marine group II/III euryarchaeote AD1000_19_F05	319
A0A075G9C4	A0A075G9C4_9ARCH	unreviewed	Ornithine carbamoyltransferase (OTCase) (EC 2.1.3.3)	OTC argF argI	uncultured marine thaumarchaeote KM3_06_A04	304
A0A075FYL2	A0A075FYL2_9EURY	unreviewed	Ornithine carbamoyltransferase (OTC, argF, argI) (EC 2.1.3.3)	OTC argF argI	uncultured marine group II/III euryarchaeote AD1000_76_E09	319
A0A075HZ97	A0A075HZ97_9EURY	unreviewed	Ornithine carbamoyltransferase (OTCase) (EC 2.1.3.3)	OTC argF argI	uncultured marine group II/III euryarchaeote KM3_85_D06	317
A0A075GVI0	A0A075GVI0_9ARCH	unreviewed	Ornithine carbamoyltransferase (OTC, argF, argI) (EC 2.1.3.3)	OTC argF argI	uncultured marine thaumarchaeote KM3_197_F10	255
A0A075FVX6	A0A075FVX6_9ARCH	unreviewed	Ornithine carbamoyltransferase (OTC, argF, argI) (EC 2.1.3.3)	OTC argF argI	uncultured marine thaumarchaeote AD1000_70_G10	304
A0A075GUU1	A0A075GUU1_9ARCH	unreviewed	Ornithine carbamoyltransferase (OTCase) (EC 2.1.3.3)	OTC argF argI	uncultured marine thaumarchaeote KM3_23_E01	302
A0A2D0R4N5	A0A2D0R4N5_ICTPU	unreviewed	ornithine carbamoyltransferase, mitochondrial isoform X1	otc	Ictalurus punctatus (Channel catfish) (Silurus punctatus)	377
A0A2D0R336	A0A2D0R336_ICTPU	unreviewed	ornithine carbamoyltransferase, mitochondrial isoform X2	otc	Ictalurus punctatus (Channel catfish) (Silurus punctatus)	314
A0A4Z2H777	A0A4Z2H777_9TELE	unreviewed	Ornithine carbamoyltransferase, mitochondrial	OTC EYF80_028868	Liparis tanakae (Tanaka's snailfish)	295
A0A218VCQ2	A0A218VCQ2_9PASE	unreviewed	Ornithine carbamoyltransferase, mitochondrial	OTC RLOC_00003735	Lonchura striata domestica (Bengalese finch)	400
Q9IAU9	Q9IAU9_ALLMI	unreviewed	Ornithine transcarbamylase	OTC	Alligator mississippiensis (American alligator)	357
A0A2I4B222	A0A2I4B222_9TELE	unreviewed	ornithine carbamoyltransferase, mitochondrial	otc	Austrofundulus limnaeus	354
A0A151NTJ7	A0A151NTJ7_ALLMI	unreviewed	Ornithine carbamoyltransferase, mitochondrial	OTC Y1Q_0000026	Alligator mississippiensis (American alligator)	354
A0A0S7EV83	A0A0S7EV83_9TELE	unreviewed	OTC (Fragment)	OTC	Poecilia reticulata (Guppy)	246
A0A2JSHIL6	A0A2JSHIL6_9EURO	unreviewed	Ornithine carbamoyltransferase OTC/ARG3	BDW42DRAFT_15683	Aspergillus prolifica (blackstripe livebearer)	246
A0A369JRZ2	A0A369JRZ2_HYPMA	unreviewed	Ornithine carbamoyltransferase, mitochondrial	OTC Hypma_008547	Aspergillus taichungensis	364
A0A319D6A3	A0A319D6A3_9EURO	unreviewed	Ornithine carbamoyltransferase OTC/ARG3	BO71DRAFT_451063	Hypsizygus marmoreus (White beech mushroom) (Agaricus marmoreus)	360
K4FTZ2	K4FTZ2_CALMI	unreviewed	Ornithine transcarbamylase	otc	Aspergillus ellipticus CBS 707.79	358
Q9IAV2	Q9IAV2_XENLA	unreviewed	Ornithine transcarbamylase	OTC XELAEV_18014763mg	Callorhinchus milii (Ghost shark)	352
B5XGX0	B5XGX0_SALSA	unreviewed	Ornithine carbamoyltransferase, mitochondrial	OTC otc	Xenopus laevis (African clawed frog)	351
					Salmo salar (Atlantic salmon)	356